Doctoral Thesis

Investigation of the two-steps clinching process for joining aluminum alloy sheets

Student Name: CHEN CHAO

Supervisor: Prof. Tohru Ishida

University: Tokushima University

Contents

1 Introduction

1.1 Background

Events such as the increased greenhouse gases and the oil crisis in 1970s become catalytic factors to a requirement for reducing the energy consumption [1]. Car safety, environmental protection and energy saving have become three major key factors to design the automobile [2], which has been given great attention of automobile manufacturer in recent years. It is important to build lightweight automotive structures to reduce the consumption of oil.

The energy used to move a car is directly proportional to its weight. The reduction in automotive weight directly contributes to reduce the energy consumption [3]. Automotive body contributes 25% to the whole weight of a car. On average, 100 kg weight reduction achieved on the automobile saves: 8 grams of CO_2 per km from the car exhaust pipe and 0.315 liter of fuel per 100 km. After analyzing 26 individual components in compact vehicles, the European Aluminum Association and University of Aachen concluded that using aluminum in some automotive parts could safely reduce vehicle body weight by up to 40 percent, resulting in 2.7 more miles per gallon of gasoline burned or approximately a 10 percent reduction in overall fuel consumption [4].

In the United States, the National Highway Traffic Safety Administration (NHTSA) and the Environmental Protection Agency (EPA) issued a joint provision in August 2012. This new regulation will have a great influence on passenger automobile to improve fuel consumption and Green House Gas (GHG) standards for cars in the year 2017 through 2025. Based on this new regulation, the emission for combined cars and trucks has to be reduced from 243 g/mile in 2017 to 163 g/mile in 2025; moreover, the fuel economy must be improved from 36.6 mpg in 2017 to 54.5 mpg in 2025. However, automobile manufacturers have to design the automobiles not only to meet requirements of the new regulations but also to compete with automotive peers. Regardless of other successful methods to improve energy economy such as development of high performance engines, fuel quality enhancement, and fuel injection system, reducing automotive weight is one of the effective approaches as by 10% weight reduction in automobile, the fuel economy improves by as much as 6-8%.

Applications of lightweight materials not only bring the potential for automobile manufacturers to reduce the car weight but also simultaneously satisfy the new regulations of fuel economy and emissions. In recent years, lightweight materials such as aluminum alloy and magnesium alloy are widely used in the automotive industry.

The use of lightweight materials also presents some new challenges in terms of manufacturing, assembling, structural properties and performance.

Welding technology is widely used to join the traditional mechanical structures. However, as shown in Fig. 1.1, spark and smoke are generated in the welding process, which will pollute the environment and damage human health. Welding technology is limited for joining some lightweight materials. For example, it is not readily suitable to join aluminum alloy sheets using welding technology. The reasons for this include:

(1) The oxidation layer on the aluminum alloy sheet surface;

(2) High thermal conductivity of the aluminum alloy;

(3) Low melting point of the aluminum alloy.

Fig. 1.1 Spark, smoke, and splash in the welding process

In order to protect the environment, some green and clean joining technologies such as mechanical clinching, self-pierce riveting, and friction stir welding are developed for joining lightweight materials. There is no smoke and spark generated in these green and clean joining technologies, which is friendly to environment.

The use of aluminum alloy and magnesium alloy is more and more because of their low density, anticorrosion and excellent machining performance. As these new materials cannot be joined effectively by conventional connecting techniques like spot welding, one of alternative joining technologies is mechanical clinching which can be used to join sheets firmly by generating an interlock. It can be used to join aluminum alloys, magnesium alloys, coated and different material sheets.

1.2 Development of mechanical clinching process

1.2.1 Mechanism of the mechanical clinching process

The main plastic deformation of the clinched joint is generated with the help of the punch, sliding sectors and fixed die [5]. The plastic deformation is used to produce a special mechanical interlock between the sheets [6]. Lambiase and Di Ilio investigated the joining process and material flow during the mechanical clinching process [7]. As shown in Fig. 1.2, with the movement of the punch, the sheets are pressed to deform downwards in the cavity surrounded by the sliding sectors and fixed dies. The force, displacement and speed of the punch are controlled accurately to get a desired clinched joint. The material flow of the sheets will drive the sliding sectors to move along the radial direction. The cavity volume surrounded by sliding sectors is enlarged with the sliding of the sectors.

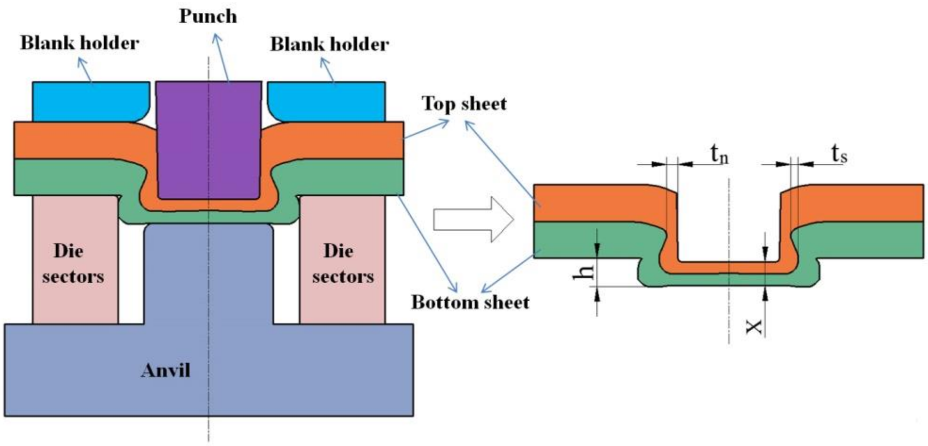

Fig. 1.2 Mechanical clinching process

There is no chemical reaction or thermal reaction generated during the mechanical clinching process [8]. Thus, mechanical clinching is a green and clean joining technology. Compared to the welding technology, the main advantages of clinching include:

(1) Environmental with no smoke and spark;

(2) Easy for process automation and monitoring;

(3) Ability to join different materials;

(4) Low quality requirements for sheet surface;

(5) Improved fatigue strength.

However, conventional mechanical clinching also has some disadvantages:

(1) Lower static strength than welding;

(2) Higher protrusion generated on the lower sheet;

(3) Inapplicability for joining brittle materials;

(4) Higher joining force.

1.2.2 Dies used in the clinching process

Though the first patent about mechanical clinching was granted in 1897, it is only in the last 30 years that the mechanical clinching has significantly developed and investigated [9]. Because of the advantages of the mechanical clinching method, several investigations about this joining technology have been carried out to widen its availability in the last decade [10, 11].

The investigation of the clinching dies is the fundamental work. The influence of clinching dies parameters, namely the punch corner radius, the punch diameter, the fixed die diameter, the fixed die depth, and the die corner radius on the mechanical properties of the clinched joint was investigated [12]. The neck thickness can be increased with larger die and punch, shallow dies and smoother corner radii. The interlock is increased by increasing punch diameter or the die depth, using dies with sharper corner radii, and reducing extensible die diameter. As shown in Fig. 1.3, Lee et al. designed mechanical clinching dies to join the aluminum alloy sheets [13]. A higher joining strength was gotten in the impact test, which proved that mechanical clinching was suitable to join components on the automobile.

(b) Clinching punch (c) Clinching die

Fig. 1.3 Clinching tools designed by Lee et al. [13]

Oudjene et al. used the Taguchi's design of experiments method to investigate the influence of clinching dies on the clinched joint resistance, as well as on its geometrical shape [14]. As shown in Fig. 1.4, different geometrical shapes were gotten in their study. The strength of the clinched joint depends on the dies geometry and can be improved by optimizing the key geometrical parameters.

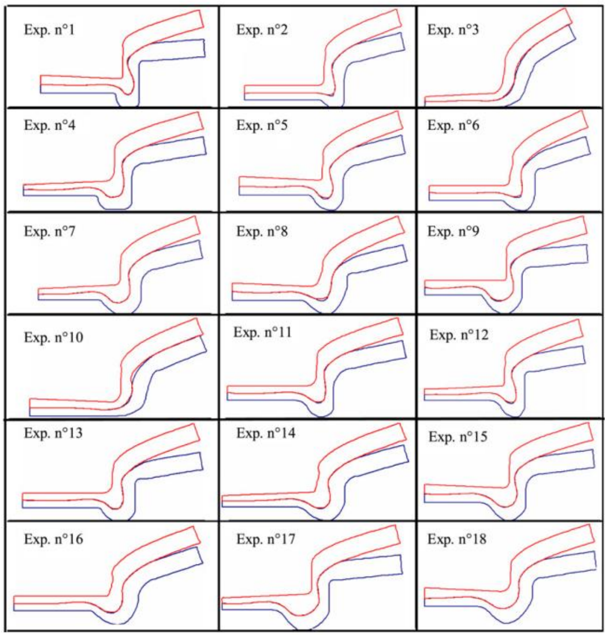

Fig. 1.4 Different geometrical shapes [14]

In order to produce clinched joint with higher strength, the clinching tools should be optimized to get optimal geometrical parameters. A response surface methodology with Moving Least-Square approximation was used to optimize the geometrical shape of the clinching dies [15]. The results showed clearly that the mechanical properties of the clinched joint were improved using the developed optimization procedure. Orthogonal design was also used to optimize the clinching process parameters, including sliding distance, bottom thickness, die depth and punch corner radius [16]. A higher joining strength of 1058 N was gotten using the optimal parameters.

1.2.3 Finite element simulation of clinching process

In order to save experimental resource and time, finite element simulation was always used to simulate the clinched joint [17, 18]. The main investigation of finite element simulation includes three aspects: (a) mechanical clinching process; (b) shearing strength and tensile strength of the joint; (c) damage and failure behavior. As shown in Fig. 1.5, a finite element model was built in LS-DYNA. It is easy to show the movement of the clinching dies using finite element simulation [19].

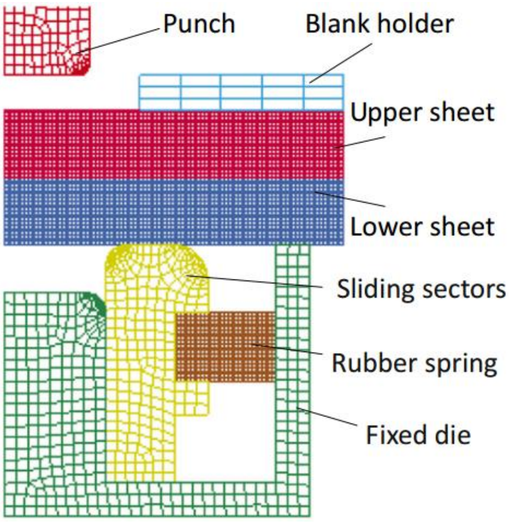

Fig. 1.5 Finite element model [19]

As shown in Fig. 1.6, He et al. also used numerical model to analyze the material flow of the mechanical clinching process [20]. The simulation results agreed well with the experimental results. Automatic remeshing was always used to prevent the mesh distortion in the finite element simulation [21]. A numerical model was also built to predict the shearing strength and tensile strength of the clinched joint [22]. The stripper mechanism, material model and interface friction are three key factors to predict the interlock region in the simulation of the clinching process. Damaging tests such as shearing test and tensile test are always used to evaluate the joining quality of the clinched joint. The clinched joint must be damaged to get the maximum strength value after the damaging test. Now, with the numerical method to predict the joining strength, many experimental resources can be saved. A numerical model for the evolution of ductile damage was built to predict the fracture behavior during the clinching process [23]. The critical regions for fracture behavior are the die-sided sheet bulge and punch-sided sheet neck. A modified Rousselier model was added into the numerical simulation to simulate the fracture behavior of the clinched joint [24]. It is feasible to use this modified Rousselier model to capture both shearing and tensile failure behavior of the clinched joint.

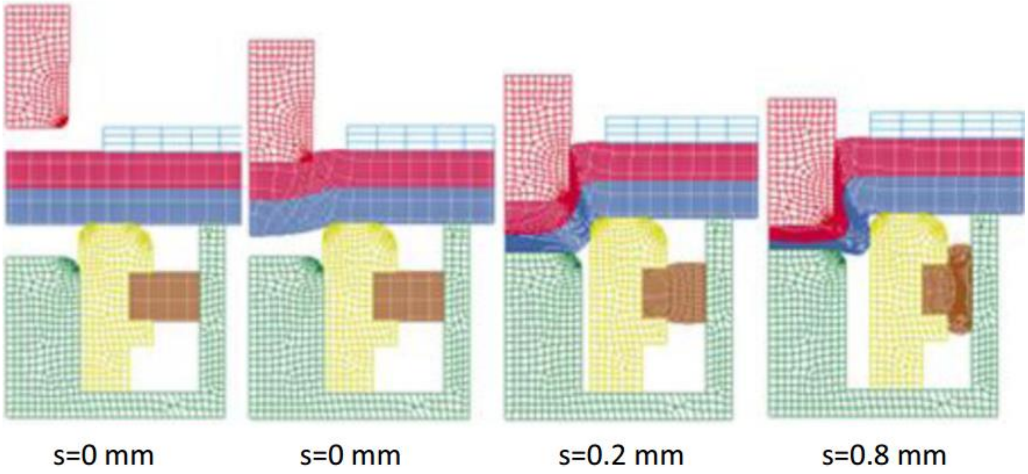

Fig. 1.6 Material flow [20]

1.2.4 Mechanical clinching process for joining different materials

Because of the different melting points, it is difficult for the different materials to be joined together effectively by the welding technology. The melting point of the material has little effect on the mechanical clinching process, so the clinching process can be used to join different materials [25]. Multi-material lightweight car body structures can be built by the clinching technology. The steel and aluminum alloy can be joined easily with a high strength by the mechanical clinching process. Meschut et al. used the mechanical clinching technology to join the boron steel sheet and aluminum alloy sheet [26]. Hörhold et al. used mechanical clinching technology to join ultra-high-strength steel and aluminum alloy to build the light-weight car body structures [27]. The joining of metal sheet and polymer sheet is a problem in the field of joining technology. It is difficult to join the metal sheet and polymer sheet by spot welding. However, the metal sheet and polymer sheet can be joined easily by mechanical clinching process. As shown in Fig. 1.7, aluminum alloy sheet can be joined together with carbon fiber reinforced polymer sheet, glass fiber reinforced polymer sheet, and other thermoplastic polymer sheets [28-32].

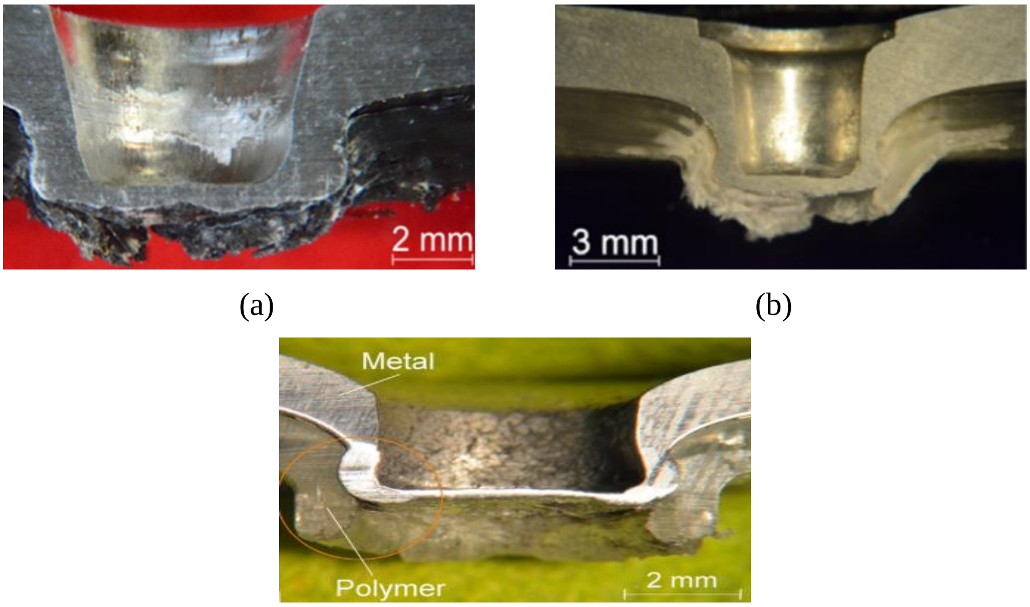

(a) (b)

(c)

Fig. 1.7 Joints with different materials: (a) carbon fiber reinforced polymer [28]; (b) glass fiber reinforced polymer [30]; (c) Transparent polystyrene [32]

It is difficult for the welding to join coated or galvanized metal sheets. Saberi et al. investigated the mechanical behavior of clinched joint with different coated thin steel sheets [33]. Abe et al. used the mechanical clinching technology to join the hot-dip coated steel sheets [34]. The thickness of the coating layer on the joined sheets was improved by the optimization of the punch and die shapes. As shown in Fig. 1.8, the joining of galvanized SAE1004 steel-to-AA6111-T4 aluminum was conducted by Jiang et al. with experimental methods [35]. The galvanized layer has little effect on the mechanical properties of the clinched joint.

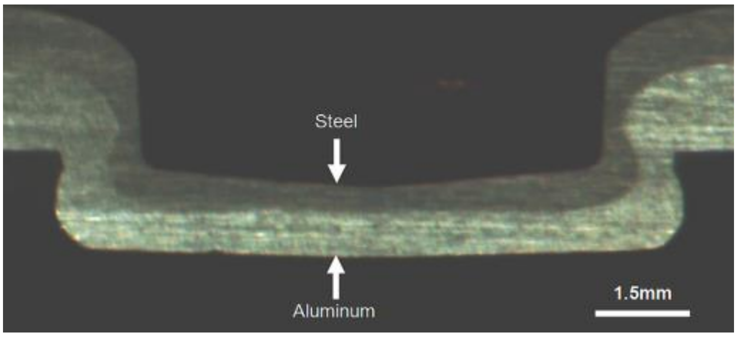

Fig. 1.8 Mechanical clinched joint of galvanized steel and aluminum [35]

1.2.5 Other clinching process

One of the main limitations for the mechanical clinched joint is represented by the stress concentration which may result in the cracks in the sheets with reduced ductility [36-38]. In order to avoid the cracks, as shown in Fig. 1.9, pre-heating process is always combined with the clinching process [39]. Another method is to use the rotating tools, which is also effective to improve the material flow [40].

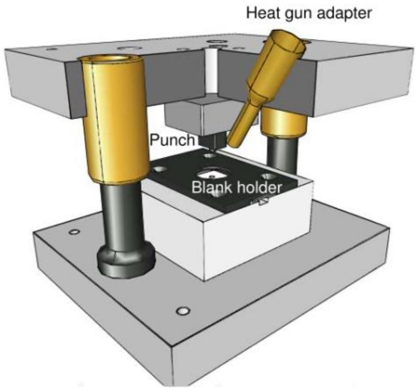

Fig. 1.9 Clinching equipment with prehearing system [36]

As shown in Fig. 1.10, there is a relatively high protrusion generated on the lower sheet, which may have an adverse effect on the following process like assembly, etc. With the exterior protrusion, it is difficult to use the clinched joint in the visible areas or functional surfaces.

Fig. 1.10 Exterior protrusion on the clinched joint

As shown in Fig. 1.11, dieless clinching process was also developed to produce clinched joint with a lower protrusion [43]. A flat counter tool, a blank holder and a punch were used as the clinching tools in the dieless clinching process. Blank holder was used to apply a defined retaining force on the sheets, and the punch was pressed into the sheets with high forming force. The sheets material flowed radially to produce a mechanical interlock between the sheets. Thus, the sheets were joined together with a high strength.

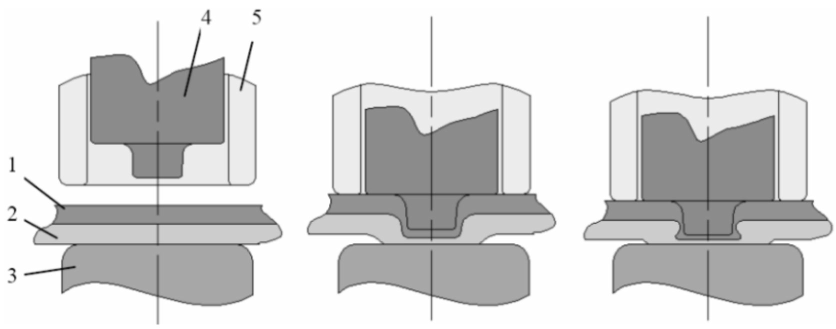

Fig. 1.11 Dieless clinching process [43]

There is still a protrusion on the lower sheet using the above methods. In order to get a flat surface, a flat clinching process was developed at the Technische Universität Chemnitz [44]. As shown in Fig. 1.12, the flat anvil could restrain the downward flow of the material, which leaded the material flow radially. With the blank holder to stamp the sheets in place, radial flow of the material was prevented. Then the material flowed opposite to the movement of the punch and moved into the space between the blank holder and punch. With the severe radial and upward material flow of the lower sheet, a reliable interlock was formed plastically [45]. Then the two sheets were joined together by the mechanical interlock [46]. With the flat anvil to restrain the material flow downward, the lower sheet contacting the flat anvil was completely flat with on exterior protrusion. As shown in Fig. 1.13, wood material and aluminum alloy also could be joined together using flat clinching process [47].

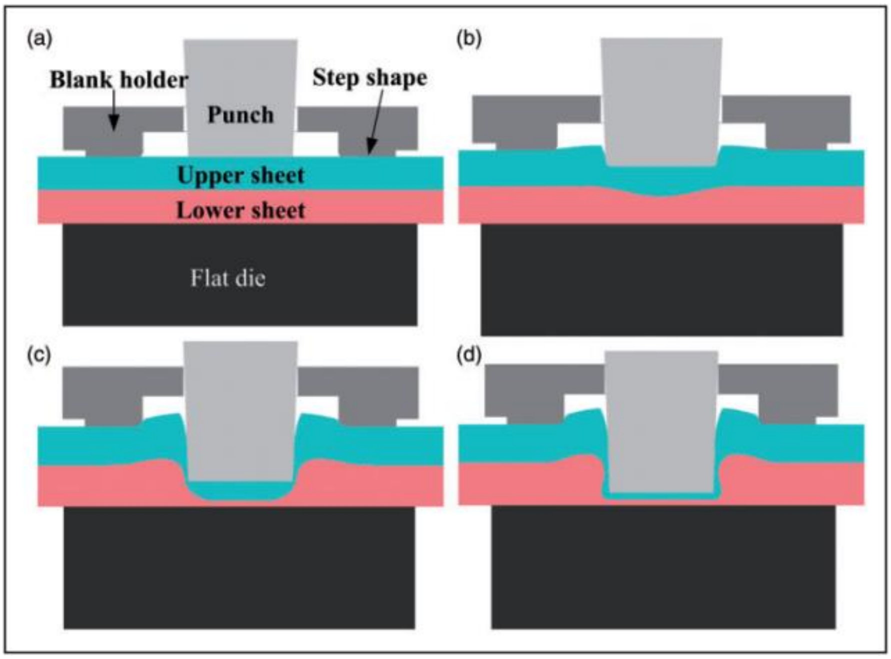

Fig. 1.12 Flat clinching: (a) location; (b) drawing; (c) protrusion; (d) filling [45]

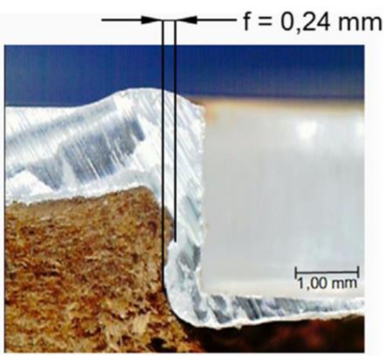

Fig. 1.13 Flat clinching of wood and aluminum alloy [47]

It is difficult for mechanical clinching process to join low-ductility materials [48]. Thus, as shown in Fig. 1.14, a new joining process, named “hole clinching”, was developed to join these materials [49]. In the hole clinching process, a hole was prepared on the low-ductility sheet [50]. The low-ductility material was taken as the lower sheet, and the ductility material was taken as upper sheet. The ductility sheet was compressed into a die cavity through the pre-punched hole in the low-ductility sheet to produce a mechanical interlock [51]. Different materials could be joined easily using this method.

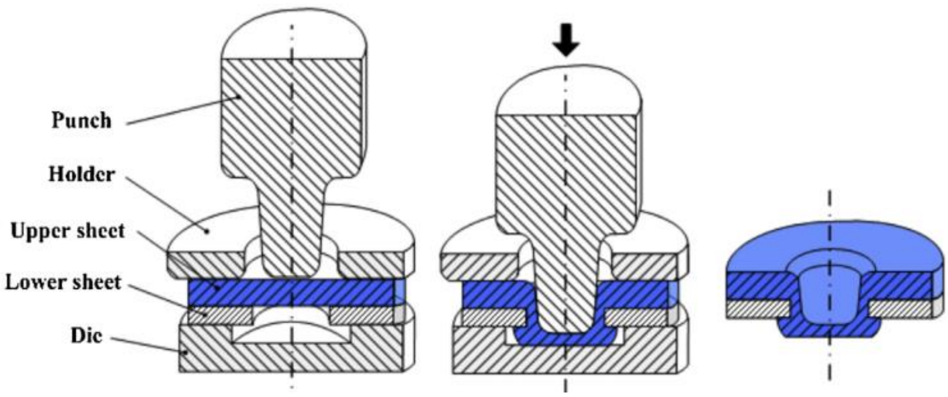

Fig. 1.14 Hole clinching process [49]

1.3 Research Objectives

Conventional mechanical clinching technology has many advantages, e.g., no damage on surface, no light and smoke, no pre-punching, energy saving and environmental protection. However, as shown in Fig. 1.15, the most obvious disadvantage of conventional clinched joint is the exterior protrusion above the sheets which could affect the wide use of mechanical clinching technology. Because of the protrusion which results in a bump jutting out of the sheet, conventional clinching technology cannot be used for visible areas where relatively flat surface is needed. In order to reduce the protrusion height, some improved clinching technologies should be proposed.

Fig. 1.15 High protrusion on the joint

In addition, the clinched joint always has a lower static strength than the self-pierce riveted joint and spot welded joint. Lower static strength means lower safety. For building the automotive structures, a joint with a higher static and fatigue strength is required. In order to enlarge the application range of the clinched joint, the strength of the joint should be increased to meet the requirement of the application. With higher static strength, the clinched joint can be used in many fields, such as automotive body, aircraft, thin-walled building structures, train, ship, and so on. It is significant to propose some methods to increase the strength of the clinched joint.

In this study, a two-steps clinching process was proposed and developed to reduce the protrusion height and increase the static strength of the clinched joint. The main research contents are as follows:

(1) Optimization of the reshaping rivet for the two-steps clinching process;

(2) Mechanical properties of the two-steps clinched joint;

(3) Effects of different parameters on the two-steps clinched joints;

(4) Comparative investigation of three different reshaping methods.

2 Optimization of the reshaping rivet for the two-steps clinching process

2.1 Mechanism of the two-steps clinching process

2.1.1 Mechanism of the first step, mechanical clinching process

In the first step, mechanical clinching process with extensible dies, a mechanical interlock is produced between the metal sheets by generating a localized deformation between the sheets in the punch-die volume [7]. The metal sheets are clinched together by being hooked with the interlock which is generated by material flow.

The first step, mechanical clinching process, is made up of four phases as shown in Fig. 2.1:

(a) the punch presses the upper sheet, and then localized plastic deformation is generated on the upper sheet and lower sheet;

(b) the generated plastic deformation continues to deform with the downward movement of the punch;

(c) the sheet material is spread radially along the radial movement of die sectors after the lower sheet moves to contact the fixed die;

(d) the sheet material continues to flow until the mechanical interlock is formed between the upper sheet and lower sheet.

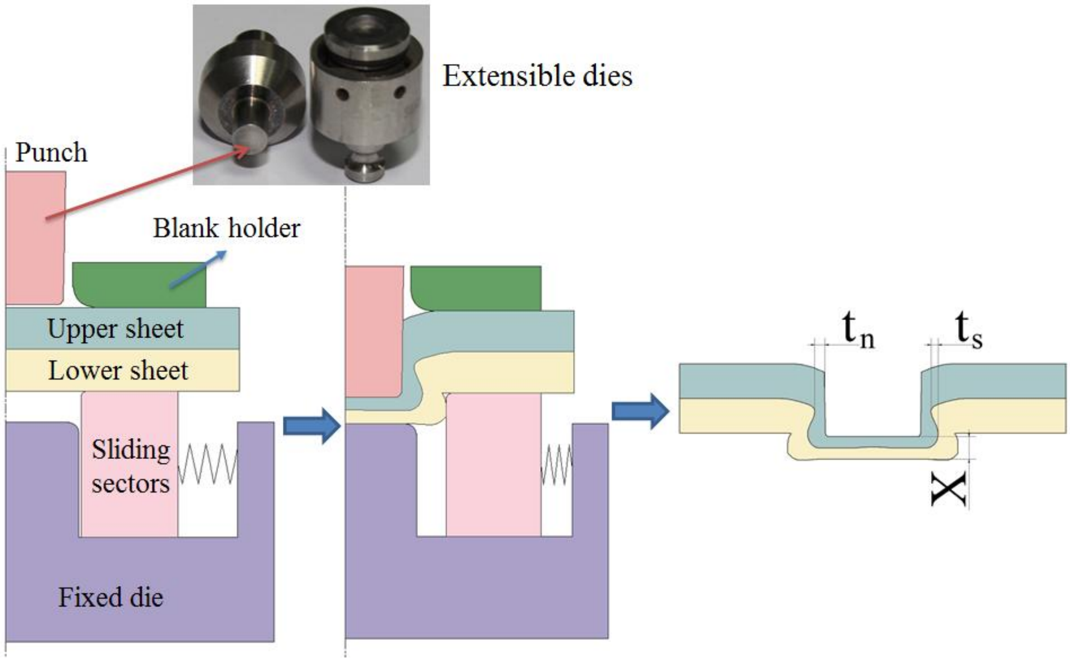

Fig. 2.1 The first step, mechanical clinching process

2.1.2 Mechanism of the second step, reshaping process

After the first step, mechanical clinching process, the clinched joint is reshaped in the second step. In the second step, reshaping process, the protrusion of the clinched joint is compressed by a pair of flat dies in a single stroke. A special clinch-rivet is used to control the material flow and increase the joining strength by being embedded in the clinched joint. The protrusion shape is modified during the reshaping process.

The second step, reshaping process with flat dies, is made up of two phases as shown in Fig. 2.2:

(a) the top flat die presses the protrusion on the lower sheet and then produces plastic deformation on the clinch-rivet and the clinched joint;

(b) the top flat die continues reshaping the protrusion until the protrusion height is decreased to the specified height.

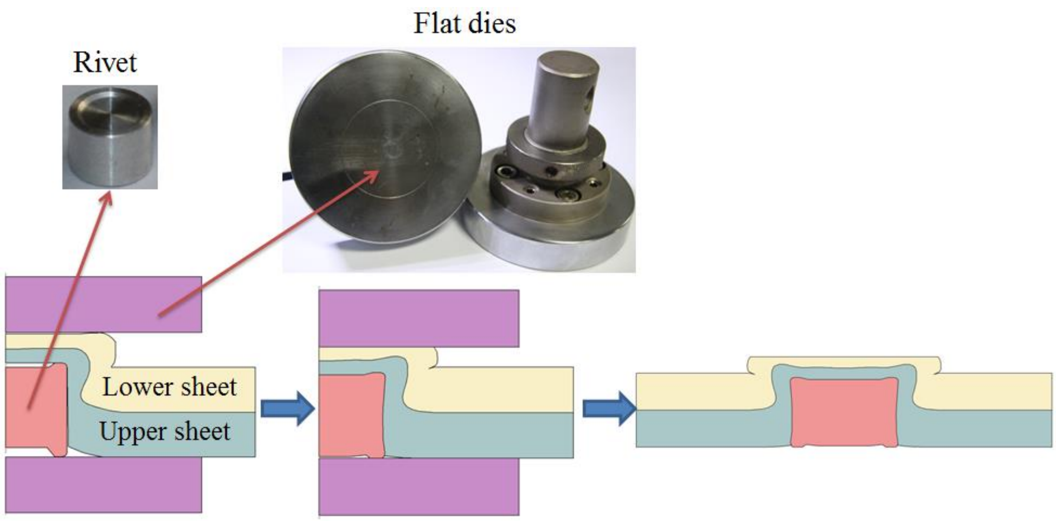

Fig. 2.2 The second step, reshaping process

2.2 Finite element simulation

2.2.1 Objective

The main objective of the finite element simulation is to investigate how geometrical parameters of the clinch-rivet affect the joining mechanical behavior. The finite element simulation will also be used to optimize the clinch-rivet in the orthogonal design.

It will take a lot of resources and time, if all the experiments with different clinch-rivet shapes are conducted. In order to save experimental resource and time, finite element simulation was taken as the research method in this study.

2.2.2 Simulation procedure

The finite element software DEFORM-2D was used to carry out the finite element simulation. It can save simulation time using 2D model with a small amount of elements. The clinched joint area is axisymmetric, which is suitable to establish a 2D axisymmetric model to simulate the two-steps clinching process and the cross-tensile separating process. The element number is decreased significantly with a shorter computing time.

The whole finite element simulation is made up of three phase: (1) the first step, mechanical clinching process, was simulated with extensible dies; (2) then the second step, reshaping process, was simulated on the basis model of the first step; (3) at last, the cross-tensile separating process was simulated to evaluate the cross-tensile strength of the two-steps clinched joint.

The first step, mechanical clinching process, is simulated with extensible dies. AL6061 was chosen as the sheet material in the simulation. The thickness of the AL6061 sheet is 2.0 mm. The sheet material was assumed as the elastic-plastic model in the software Deform 2D. Mechanical properties of AL6061 used in this study are presented in Table 2.1.

Table 2.1 Mechanical properties of AL6061

Material	Yield stress (MPa)	Elastic modulus (GPa)	Poisson's ratio (-)
AL6061	207.9	67.6	0.33

Instron 5982 testing machine was used to carry out the tensile tests to get the mechanical properties of AL6061. Quadrilateral elements were used to mesh the aluminum alloy sheets with 5980 elements and 6348 nodes in the numerical model. Automatic remeshing method was also applied to prevent the mesh distortion in the finite element simulation [21]. The punch, blank holder, sliding die sectors and fixed die were taken as rigid [52]. The geometry parameters of the extensible dies used in the mechanical clinching process is shown in Fig. 2.3. The moving type of the die sectors was taken as the sliding die. It can slide with the material flow along the fixed die. The friction condition between the upper sheet and lower sheet was modeled by assuming a coulomb friction as μ=0.3. The friction coefficient between the sheets and the dies was assumed as 0.15. The friction coefficient was assumed as 0.15 between metal sheet and blank holder as well as between metal sheet and punch. The punch with a velocity of 0.5 mm/s moved to compress the sheets until the bottom thickness of the produced joint was decreased to 1.3 mm. After the mechanical clinching process, the clinched joint was produced with a protrusion height of 1.6 mm. Spring back can be ignored in the finite element simulation [18].

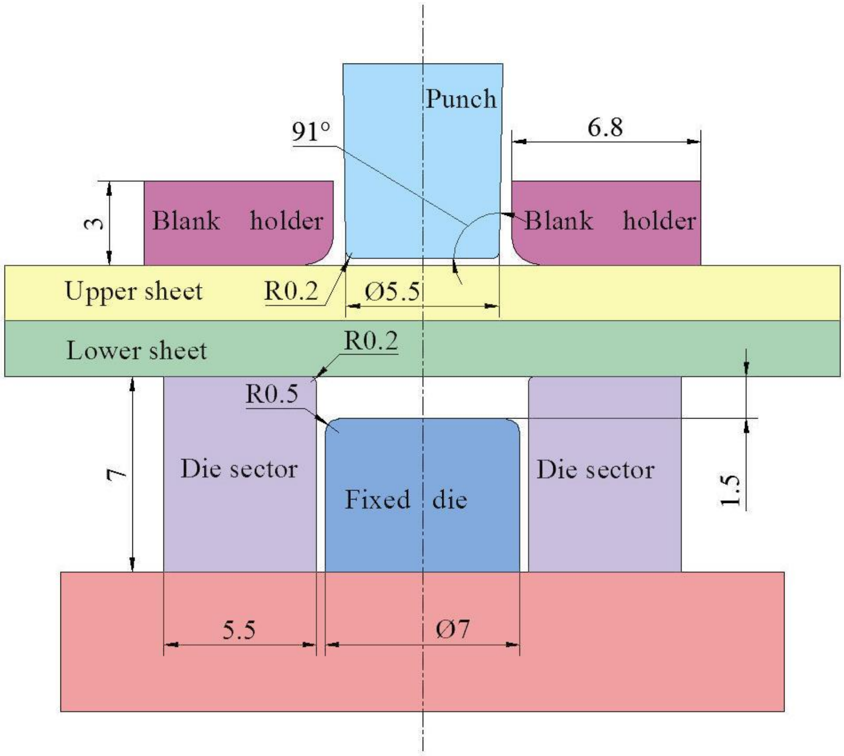

Fig. 2.3 Geometrical parameters of the extensible dies

After the simulation of the first step, mechanical clinching process, the second step, reshaping process, was simulated with a clinch-rivet. The material of the clinch-rivet was set as Al6061. Quadrilateral elements were also used to mesh the clinch-rivet with 1116 elements and 1184 nodes in the numerical model. The bottom flat die and the top flat die were assumed as rigid, while the material of the clinch-rivet was assumed as elastic-plastic. The thickness of the flat die is 3 mm and the diameter is 24 mm. The friction coefficient between the upper sheet and lower sheet was assumed as 0.3 with a coulomb friction model. The friction coefficient between the sheets and the dies was assumed as 0.15. The friction coefficient between the bottom die and the rivet was assumed as 0.15, while between the upper sheet and the clinch-rivet was assumed as 0.3. The top flat die was controlled to move downward to compress the protrusion with a velocity of 0.05 mm/s, and the bottom flat die was fixed. After the protrusion height of the joint was reduced from 1.6 to 1.0 mm, the top flat die was stopped.

The cross-sectional geometry of the clinch-rivet is shown in Fig. 2.4. Two different pits are machined in the upper surface and lower surface of the cylindrical rivet, respectively. In order to embed the clinch-rivet in the pit on the clinched joint, the clinch-rivet diameter should not be machined larger than the pit diameter, and the clinch-rivet should not be machined larger than the pit depth. Thus the clinch-rivet diameter is made as the same as the pit diameter with 5.5 mm. The clinch-rivet should be made shaft alignment. Because of the same diameter, the clinch-rivet can be embedded at the bottom of the pit. The lower surface of the clinch-rivet should contact the bottom die, and the upper surface of the clinch-rivet should contact the pit bottom to control the material flow. Thus the height of the clinch-rivet is 4.2 mm which is the same as the depth of the pit. The fillet of the clinch-rivet is is consistent with the punch fillet which is 0.2 mm. In the second step, reshaping process, the pit with diameter 'd_1' in lower surface of the clinch-rivet is facing the lower flat die, and the pit with diameter 'd_2' in upper surface of the clinch-rivet is facing the sheet.

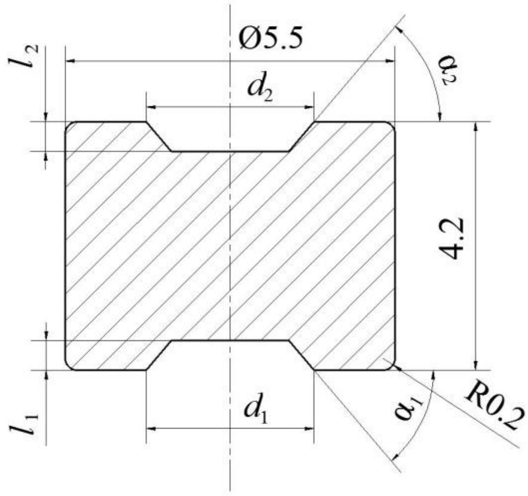

Fig. 2.4 Cross-sectional geometry of the reshaping rivet

The third phase in the simulation is cross-tensile separating process. Static cross-tensile and tension-shearing tests are always performed to evaluate the joining strength of the clinched joint. As pointed out by Coppieters et al., cross-tensile strength of the joint is always much lower than the tension-shear strength [10]. Many clinched joints were failed in the use because of the lower cross-tensile strength. Therefore, cross-tensile strength of the clinched joint is taken as one of the most important evaluation index in the numerical simulation.

The finite element model which is used for performing the cross-tensile separating process of the two-steps clinched joint is shown in Fig. 2.5. The speed of the cross-tensile separating process was set as 2 mm/min. An upward movement was set on the ambient edge of the upper sheet, and the bottom part of the lower sheet was fixed. The maximum force needed for the upward movement in the cross-tensile separating process could be taken as the cross-tensile strength of the two-steps clinched joint.

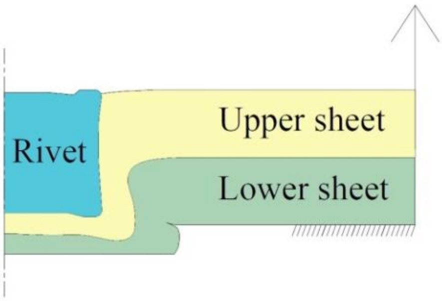

Fig. 2.5 Schematic drawing of the cross-tensile separation

2.2.3 Main simulation results

The whole finite element simulation including mechanical clinching process, reshaping process and cross-tensile separating process should be performed in succession to make sure the whole simulation conditions are consistent.

The first step, mechanical clinching process, was simulated first in the software DEFORM-2D. The simulation results of the first step, mechanical clinching process with extensible dies, are shown in Fig. 2.6. As can be seen, the main plastic deformation occurred at the bottom of the clinched joint. In the end of the clinching process, a mechanical interlock is produced between the two sheets.

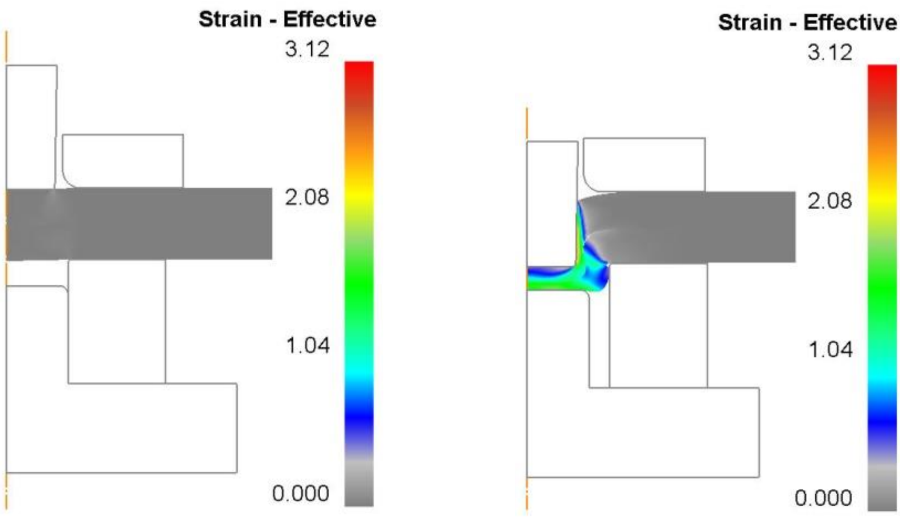

(a) (c)

Fig. 2.6 Numerical results of mechanical clinching

The second step, reshaping process, was continued to be simulated after the first step by changing the dies and the speed of the top die. The final geometry and deformation of the clinched joint produced in the first step can be inherited smoothly in the second step. The simulation results of the reshaping process with a clinch-rivet are shown in Fig. 2.7.

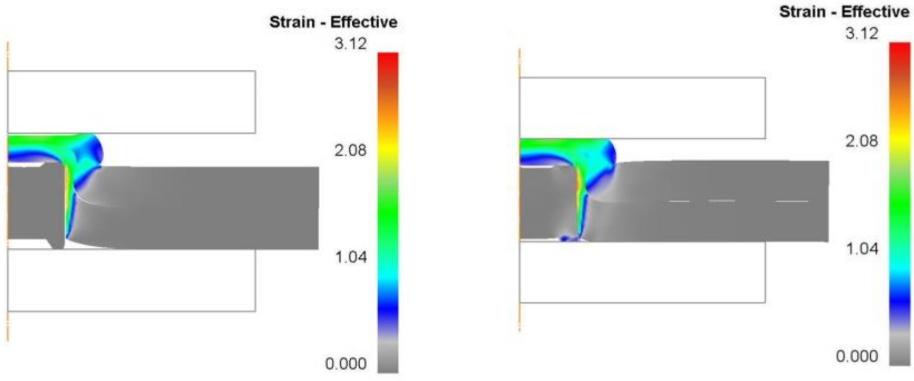

(a) (c)

Fig. 2.7 Numerical results of reshaping

In the last phase, the cross-tensile separating of the two-steps clinched joint was simulated. The simulation results of the cross-tensile separating process are shown in Fig. 2.8.

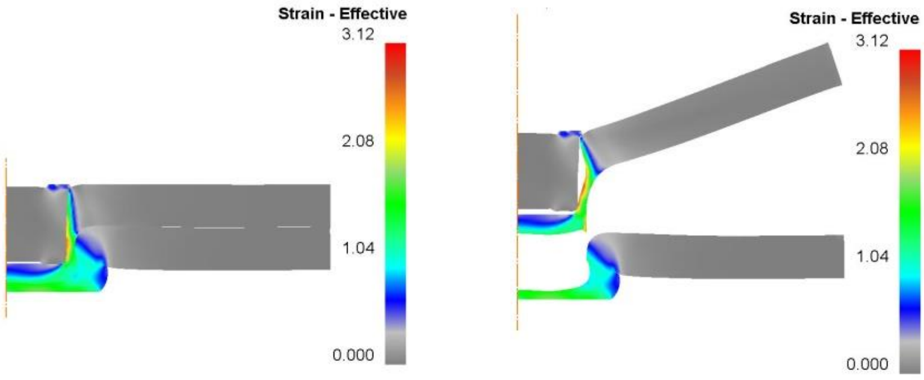

(a) (c)

Fig. 2.8 Numerical results of cross-tensile separation

2.3 Geometrical parameter optimization of the clinch-rivet

In order to get the optimized geometrical parameters of the clinch-rivet to increase the joining strength and reduce the protrusion height, an effective optimum design method is needed in this study. In the process of clinching, many different levels and factors should be taken into consideration. Orthogonal design is widely used to study multiple levels and multiple factors, which is suitable to be used for optimizing geometrical parameters of the clinch-rivet. This design method can make each design highly representative with the two advantages of uniformly dispersed, neat and comparable. Representative points from the comprehensive designs are selected in the orthogonal design, which can help to reflect the effects of different levels of different factors on the final design result. By selecting representative experimental scheme, it takes less time in the orthogonal design.

In order to increase the joining strength, the cross-tensile strength of the two-steps clinched joint is taken as the major concern factor in the optimizing process of geometrical parameters of the clinch-rivet. As shown in Fig. 2.9 (indicated by the arrows), the material around the upper and lower pits of the clinch-rivet will flow radially to enlarge the interlock and neck thickness in the second step, reshaping process. In order to achieve the specified material flow, geometrical parameters of the clinch-rivet mainly include the depths (l_1 and l_2), the tapers (α_1 and α_2) and the diameters (d_1 and d_2) of the upper and lower pits in the surfaces of the clinch-rivet in orthogonal design. As presented in Table 2.2, six five-level factors are considered in the orthogonal array, which is used to optimize geometry parameters of the clinch-rivet. These factors and levels are more helpful to increase the strength of the two-steps clinched joint. According to the designed orthogonal array shown in Table 2.3, in order to get the optimal geometrical parameters, 25 groups of different geometrical parameter combinations of the clinch-rivet should be investigated and simulated. In order to save simulation time and improve efficiency, the unfavorable interdependency between geometrical parameters of the clinch-rivet was ignored in the orthogonal design [18]. If the interdependency between different geometrical parameters is considered in the design, the orthogonal design procedure will be more complex. It will take a lot of resources and time, if many factors are considered in the orthogonal array. Thus, six five-level factors are considered in the orthogonal array.

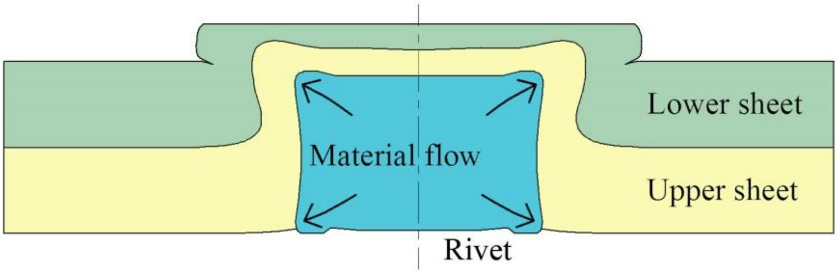

Fig. 2.9 Material flow of the reshaping rivet

Table 2.2 Geometrical parameters and levels of the reshaping rivet

Level	A d_1 (mm)	B α_1 (°)	C l_1 (mm)	D d_2 (mm)	E α_2 (°)	F l_2 (mm)
1	2.8	35	0.2	2.8	35	0.2
2	3.2	40	0.3	3.2	40	0.3
3	3.6	45	0.4	3.6	45	0.4
4	4.0	50	0.5	4.0	50	0.5
5	4.4	55	0.6	4.4	55	0.6

Table 2.3 Results of orthogonal design

No.	A	B	C	D	E	F	Cross-tensile strength (N)
1	1	1	1	1	1	1	1092.4
2	1	2	2	2	2	2	1096.3
3	1	3	3	3	3	3	1095.7
4	1	4	4	4	4	4	1097.0
5	1	5	5	5	5	5	1102.5
6	2	1	2	3	4	5	1099.9
7	2	2	3	4	5	1	1113.9
8	2	3	4	5	1	2	1115.5
9	2	4	5	1	2	3	1111.3
10	2	5	1	2	3	4	1102.8
11	3	1	3	5	2	4	1111.0
12	3	2	4	1	3	5	1113.6
13	3	3	5	2	4	1	1112.9
14	3	4	1	3	5	2	1111.6
15	3	5	2	4	1	3	1116.5
16	4	1	4	2	5	3	1116.2
17	4	2	5	3	1	4	1118.8
18	4	3	1	4	2	5	1122.3
19	4	4	2	5	3	1	1136.3
20	4	5	3	1	4	2	1124.9
21	5	1	5	4	3	2	1118.4
22	5	2	1	5	4	3	1121.0
23	5	3	2	1	5	4	1121.0
24	5	4	3	2	1	5	1137.9
25	5	5	4	3	2	1	1138.6

Range analysis was carried out to analyze how much geometrical parameters of the clinch-rivet affect the cross-tensile strength according to the numerical results of the finite element simulation. Table 2.4 shows the results of the range analysis. The effect curves of main geometrical parameters on the cross-tensile strength are shown in Fig. 2.10. The diameter ‘d_1’ of the upper pit in the surface of the clinch-rivet has the largest range value which means that it has the greatest effect on the cross-tensile strength, so it is taken as the most important parameter which needs to be considered first in the design.

Table 2.4 Range analysis

	A	B	C	D	E	F
	d_1 (mm)	α_1 (°)	l_1 (mm)	d_2 (mm)	α_2 (°)	l_2 (mm)
K_1	5483.9	5537.9	5550.1	5563.2	5581.1	5594.1
K_2	5543.4	5563.6	5570	5566.1	5579.5	5566.7
K_3	5565.6	5567.4	5583.4	5564.6	5566.8	5560.7
K_4	5618.5	5594.1	5580.9	5568.1	5555.7	5550.6
K_5	5636.9	5585.3	5563.9	5586.3	5565.2	5576.2
k_1	1096.78	1107.58	1110.02	1112.64	1116.22	1118.82
k_2	1108.68	1112.72	1114	1113.22	1115.9	1113.34
k_3	1113.12	1113.48	1116.68	1112.92	1113.36	1112.14
k_4	1123.7	1118.82	1116.18	1113.62	1111.14	1110.12
k_5	1127.38	1117.06	1112.78	1117.26	1113.04	1115.24
R	30.6	11.24	6.66	4.62	5.08	8.7

K_i (i=1,2,3,4,5): total cross-tensile strength value in the 'i–th'level of each factor,

k_i (i=1,2,3,4,5): average cross-tensile strength value in the 'i–th' level of each factor, $k_i = K_i/5$,

R: maximum range value of cross-tensile strength.

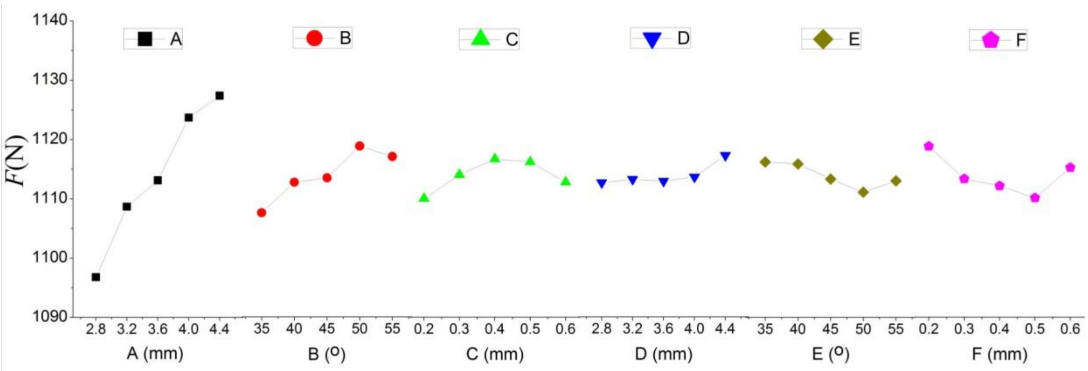

Fig. 2.10 Effect of parameter levels on cross-tensile strength

As shown in Fig. 2.10, the cross-tensile strength can be increased with the further increase in factor 'A'. The pit machined on the clinch-rivet surface is applied to enlarge the interlock and neck thickness in the second step, reshaping process. The materials around the upper pit and lower pit in the surfaces of the clinch-rivet will flow radially to enlarge the neck thickness and interlock. The factor 'A' was set to 4.4, 4.0, 3.6, 3.2 and 2.8 mm, respectively. The increase gradient of factor 'A' was set to 0.4 mm. The next value of diameter 'A' will be set as 4.8 mm. However, this is a large parameter for the factor 'A'. If the diameter 'A' is set as 4.8 mm, the material around the pits will not flow to the right direction. As shown in Fig. 2.11, a clinch-rivet with a larger pit is simulated in the second step, reshaping process. As shown in Fig. 2.11 (b), the material around the pits will flow to the direction indicated by the red arrow with the movement of the upper flat die. This material flowing direction cannot contribute to enlarge the neck thickness and interlock in the second step, reshaping process.

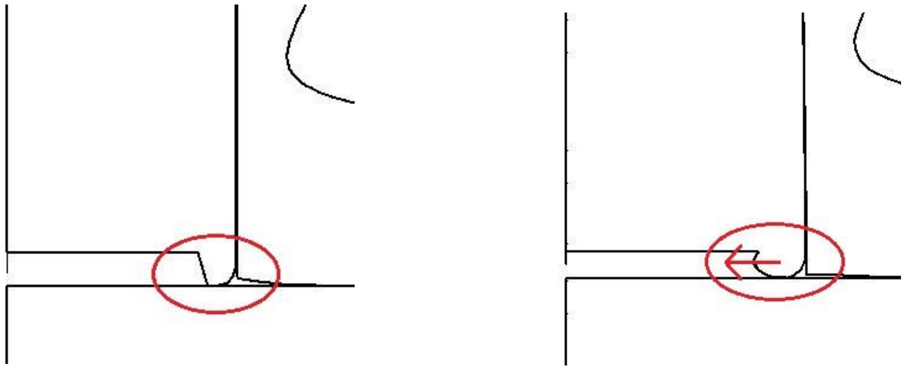

(a) (b)

Fig. 2.11 Material flow of the clinch-rivet with a larger pit

Range analysis may not distinguish the data fluctuation caused by the deviation. Thus, analysis of variance (ANOVA) is used to distinguish the data fluctuation in this study. The results of ANOVA are shown in Table 2.5. The equations to calculate the values are shown as follows:

$$k = \frac{k_1 + k_2 + k_3 + k_4 + k_5}{5} \tag{1}$$

$$Sum = 5 \times [(k_1 - k)^2 + (k_2 - k)^2 + (k_3 - k)^2 + (k_4 - k)^2 + (k_5 - k)^2] \tag{2}$$

$$\text{Mean square} = \frac{Sum}{DOF} \tag{3}$$

$$F = \frac{Sum}{Sum_F} \tag{4}$$

Where k is the average value of the k_i (i=1,2,3,4,5), DOF is the degree of freedom, Sum_F is the sum of squares of F factors.

It can be noticed that factor 'A' and factor 'B' have significant effect ($F > F_{0.05}$, $P < 0.05$) on the cross-tensile strength of the two-steps clinched joint, while factor 'C', factor 'D', factor 'E', and factor 'F' have slight effect ($F < F_{0.05}$, $P > 0.05$). However, main geometrical parameters of the clinch-rivet include the depths (l_1 and l_2), the diameters (d_1 and d_2) and the tapers (α_1 and α_2) of the upper pit and lower pit in the surfaces of the clinch-rivet in the orthogonal design. Every geometrical parameter has an effect on the joining strength of the two-steps clinched joint and needs an optimal value. ANOVA method only can show that the factor 'A' and factor 'B' have significant effect on cross-tensile strength, which is not effective to mean that the optimal combination of the geometrical parameters is A5B4. If only two geometrical parameters ('A' and 'B') are considered in the designing combination, the combination will not be the optimal designing combination which can get the maximum cross-tensile strength.

Table 2.5 Analysis of variance

Factors	Sum of squares	DOF	Mean square	*F* value
A	2993.48	4	748.37	68.47
B	378.49	4	94.62	8.66
C	146.20	4	36.55	3.34
D	71.87	4	17.97	1.64
E	90.13	4	22.53	2.06
F	43.70	4	10.93	1

$F_{0.05}$=6.39.

The order of the importance of these geometrical parameters which has been verified by the results in ANOVA and range analysis is the diameter (d_1) of the lower pit, the taper (α_1) of the lower pit, the depth (l_2) of the upper pit, the depth (l_1) of the upper pit, the taper (α_2) of the upper pit, and the diameter (d_2) of the lower pit. As shown in Table 2.6, the optimal geometrical parameters combination of the clinch-rivet is $A_5B_4C_3D_5E_1F_1$. The optimal value of each parameter chosen in this study is the value which can contribute to achieve the highest cross-tensile strength in Fig. 2.10.

Table 2.6 Best combination of the rivet geometrical parameters

	A	B	C	D	E	F
	d_1 (mm)	α_1 (°)	l_1 (mm)	d_2 (mm)	α_2 (°)	l_2 (mm)
optimization	4.4	50	0.4	4.4	35	0.2

2.4 Experiment

2.4.1 Experimental procedure

The two-steps clinching experiment, was carried out using the Al6061 sheet with a nominal thickness of 2.0 mm. The Al6061 sheets used in the experiments were cut into rectangle strips (25 mm×80 mm). The whole two-steps clinching experiment consisted of two steps: firstly, the mechanical clinching experiment was carried out with extensible dies; then the second step, reshaping experiment, was carried out on the basis of the conventional clinched joint.

The extensible dies used in the mechanical clinching experiment are shown in Fig. 2.12. A mechanical clinching machine produced by express company was applied to carry out the mechanical clinching experiment.

The geometrical parameters and shapes of the extensible dies used in the experiment are consistent with the dies model used in the finite element simulation. The punch speed in the clinching process was set as 0.5 mm/s. When the bottom thickness of the mechanical clinched joint was decreased to 1.3 mm, the punch was stopped at once.

Fig. 2.12 Extensible dies

The two flat dies used in the second step, reshaping experiment, are shown in Fig. 2.13. A hydraulic servo press with 160 kN was adopted to carry out the reshaping experiment. The surfaces of the dies which contact the aluminum alloy sheets are flat, which is suitable to reshape the protrusion.

Fig. 2.13 Reshaping dies

According to the numerical simulation, the clinch-rivet with optimal geometrical parameters was used in the second step, reshaping experiment, as shown in Fig. 2.14. Five aluminum alloy clinch-rivets were weighed. The average weight of the five clinch-rivets is 0.243 g.

The top die speed in the reshaping experiment was set to 0.05 mm/s. When the protrusion height was decreased to 1.0 mm, the top die was stopped at once.

Fig. 2.14 Reshaping rivet

Static cross-tensile test and tension-shearing test are always used to evaluate the joining quality of the clinched joint [53]. After the two-steps clinching process, the static cross-tensile test and tension-shearing test of the two-steps clinched joint were carried on Instron 5982 testing machine. The joining specimens used in static cross-tensile test and tension-shearing test are illustrated in Fig. 2.15. The separating speeds in the static cross-tensile test and tension-shearing test were set to 2 mm/min.

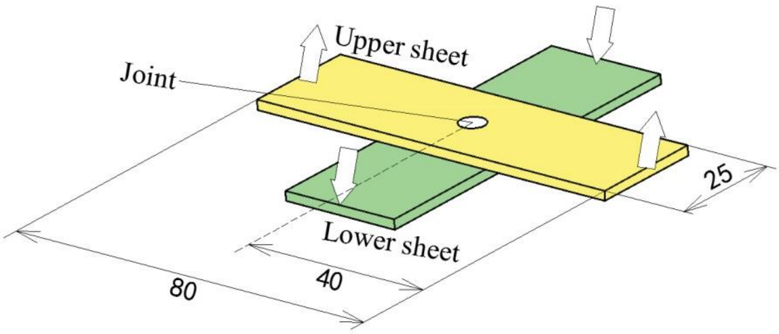

(a)

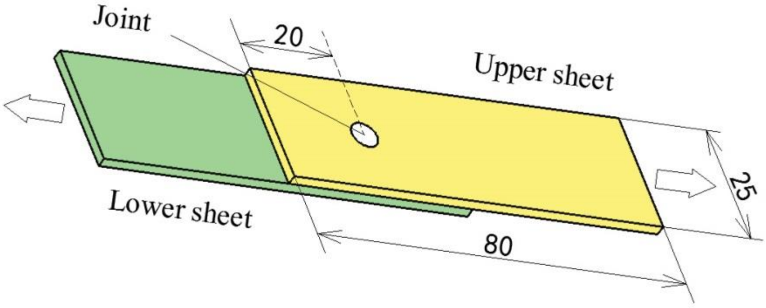

(b)

Fig. 2.15 Joined sheets used for cross-tensile and tension-shearing tests: (a) Specimen used for cross-tensile test; (b) Specimen used for tension-shearing test

2.4.2 Results and discussion

After the second step, reshaping process, the protrusion height of the two-steps clinched joint was decreased to 1.0 mm. The comparison of the conventional clinched joint (before the reshaping process) and reshaped joint (after the reshaping process) is shown in Fig. 2.16.

Fig. 2.16 Comparison of clinched joint and reshaped joint

The cross-sectional profile comparison between the experimental result and simulation result is suitable to be used for validating the numerical model [20]. The cross-sectional profile comparison of the two-steps clinched joint between the experimental result and simulation result is shown in Fig. 2.17. The geometrical parameters comparison of the experimental result and simulation result is shown in Table 2.7. As can be seen, the errors of the experimental result and simulation result in evaluation of the geometrical parameters are less than 8%. The final comparison of the experimental and numerical cross-tensile load-displacement curve is shown in Fig. 2.18. The numerical curve agrees fairly well with experimental curve.

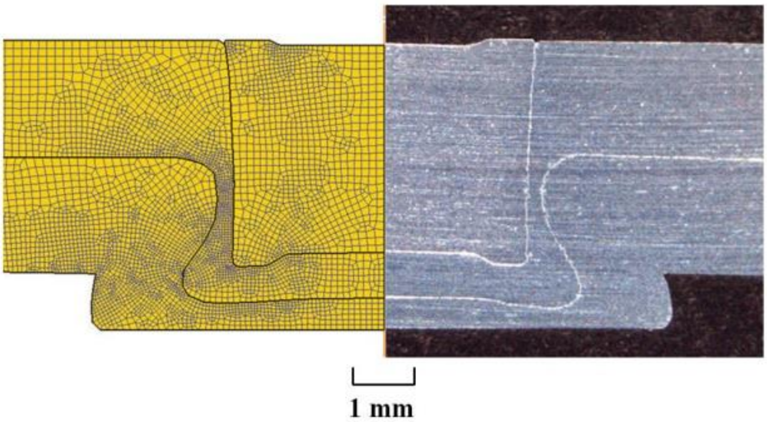

Fig. 2.17 Cross-section comparison

Table 2.7 Comparison of the geometrical parameters

	Neck thickness (mm)	Undercut (mm)	Bottom thickness (mm)
Numerical result	0.346	0.663	1.272
Experimental result	0.321	0.692	1.278

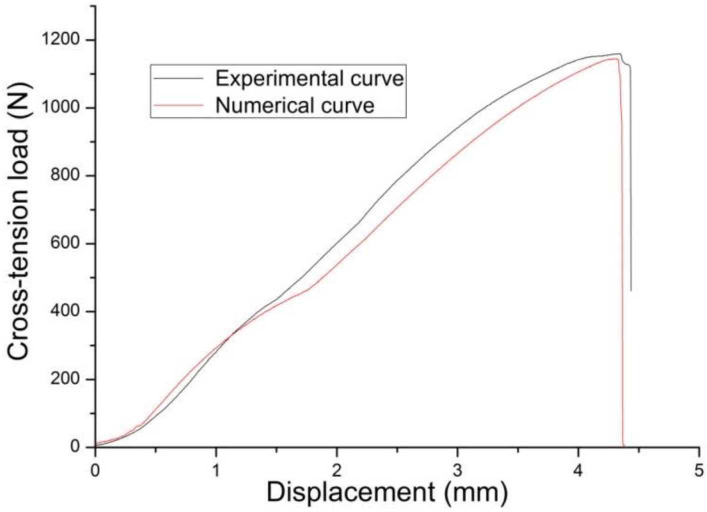

Fig. 2.18 The comparison of the numerical and experimental curve

Five groups of cross-tensile tests are carried out to get the experimental cross-tensile strengths of conventional clinched joints and two-steps clinched joints. The cross-tensile strengths of the conventional clinched joints and two-steps clinched joints are listed in Table 2.8. The average cross-tensile strength of the conventional clinched joints (before reshaping process) is 957.9 N, while the average cross-tensile strength of the two-steps clinched joints (after reshaping process) is 1154.9 N. Compared with the conventional clinched joints before reshaping, the average cross-tensile strength of the two-steps clinched joints is increased by 20.6%.

Table 2.8 Cross-tensile strengths of clinched joints and reshaped joints

	Cross-tensile strength (N)					
	Test 1	Test 2	Test 3	Test 4	Test 5	Average
Before reshaping	932.6	973.7	955.2	952.1	976.1	957.9
After reshaping	1159.8	1144.3	1178.6	1101.8	1189.9	1154.9

Due to the experiment error, some numerical data in Table 2.3 are also within the limits of experimental data of table 8. Each experimental test may generate experimental errors, thus five groups of static cross-tensile tests are carried out to guarantee the accuracy of the experimental result of the average cross-tensile strength. The average static cross-tensile strength is more representative to evaluate the joining quality of the joint. The average cross-tensile strength of the two-steps clinched joint is 1154.9 N. All the numerical results in Table 3 are smaller than the experimental value 1154.9 N.

Five groups of tension-shearing tests are carried out to get the average tension-shearing strengths of the joints. The tension-shearing strengths of the conventional clinched joints and two-steps clinched joints are listed in Table 2.9. The average tension-shearing strength of the two-steps clinched joints is 2757.3 N, while the average tension-shearing strength of the conventional clinched joints is 1229.4 N. The average tension-shearing strength of the two-steps clinched joints after reshaping is increased by 124.3% compared with the conventional clinched joint before reshaping.

Table 2.9 Tension-shearing strengths of the clinched joints and the reshaped joints

	Tension-shearing strength (N)					
	Test 1	Test 2	Test 3	Test 4	Test 5	Average
Before reshaping	1217.4	1220.3	1233.8	1223.1	1252.2	1229.4
After reshaping	2683.2	2703.9	2798.1	2812.9	2788.5	2757.3

The numerical cross-tensile strength of the conventional clinched joint is 949.2 N and the average experimental cross-tensile strength is 957.9 N. The error for the evaluation of the cross-tensile strength of the conventional clinched joint is 0.91%. The numerical cross-tensile strength of the two-steps clinched joint is 1144.8 N, and the average experimental cross-tensile strength is 1154.9 N. The error for the evaluation of the cross-tensile strength of the two-steps clinched joint is 0.87%. The comparison shows that the experimental results and numerical results are in good agreement.

The material around the upper pit and lower pit in clinch-rivet will flow radially to enlarge the interlock in the second step, reshaping process, as shown in Fig. 9. In the second step, reshaping process, the protrusion was reshaped by the top flat die. As shown in Fig. 2.19, the protrusion material will flow downward to the neck area as indicated by the green arrows. The material around the upper pit and lower pit of the clinch-rivet can make the clinch-rivet material to be gathered in the neck area as indicated by the red arrows. This can contribute to enlarge the neck thickness. The joining strength of the two-steps clinched joint is increased by increasing the interlock and neck thickness. In the static strength tests, the clinch-rivet can also bear the tensile force to increase the joining strength of the two-steps clinched joint, and the clinch-rivet will also deform to absorb more energy.

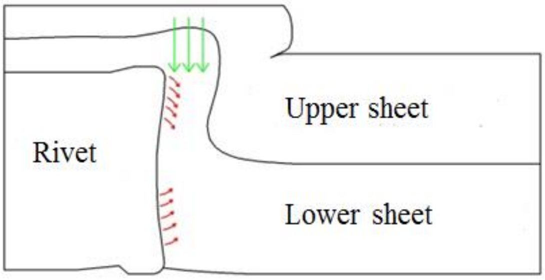

Fig. 2.19 Material flow

2.5 Conclusions

In order to reduce the protrusion height and increase the strength of clinched joints, a two-steps clinching method using a rivet to reshape the clinched joint was put forward in the study. The AL6061 sheets with nominal thickness of 2.0 mm were used to study the reshaping method. The reshaping method can be a helpful supplement of conventional mechanical clinching. The conclusions can be drawn as follows:

1. The numerical results and experimental results are in good agreement and the error in the evaluation of the cross-tensile strength is less than 1%.

2. The best combination of the reshaping rivet geometrical parameters was gotten in terms of the cross-tensile strength by orthogonal design.

3. Factor A and factor B have significant effects on cross-tensile strength and the order of the factors' importance is A (d_1), B (α_1), F (l_2), C (l_1), E (α_2), and D (d_2).

4. In the experiment, when the protrusion height of the joint was reduced to 1.0 mm, the average cross-tensile strength was increased from 957.9 to 1154.9 N, and the average tension-shearing strength was increased from 1229.4 to 2757.3 N.

3 Mechanical properties of the two-steps clinched joint

3.1 Forming force and geometrical parameters

3.1.1 Analysis of forming force

The first step in the two-steps clinching process is the conventional mechanical clinching process, which behaves like a metal bulk forming process. The interlock between the aluminum alloy sheets is generated by the joining force on the punch. Lambiase and Di Ilio investigated the effect of different joining forces on the material flow of the conventional clinched joint [7]. The interlock may fail to be generated, if the joining force is too small. Joining force is one of the most important parameters in the conventional clinching process.

Five groups of joining forces are shown in Fig. 3.1. The five joining force-displacement curves of the conventional clinching process have very high consistency in trend and shape, which means that the repeatability of the conventional mechanical clinched joints is very high. According to the joining force-displacement curves, the joining force in the conventional clinching process is greatly influenced by the punch displacement. In this study, the average joining force of the conventional clinching process is 2958 N.

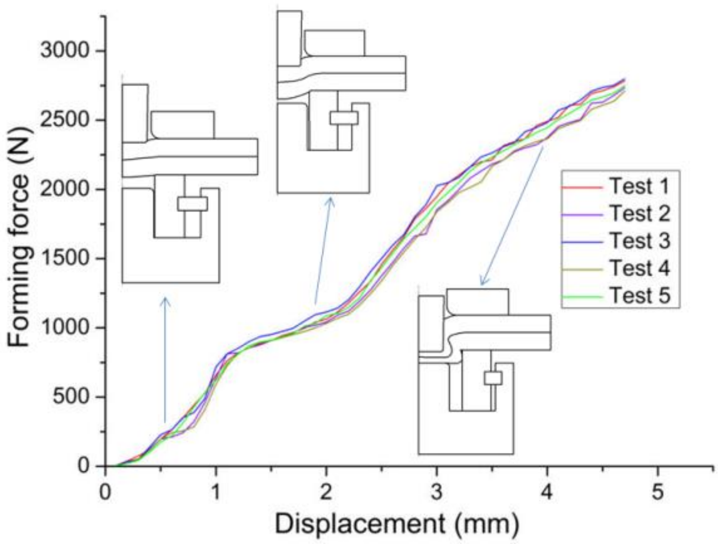

Fig. 3.1 The force-displacement curves of the conventional mechanical clinching

In the second step, reshaping process, the conventional clinched joint was reshaped by compressing the protrusion with a special clinch-rivet. The conventional clinched joints were reshaped under different reshaping forces on the top flat die. In order to make the comparison easily, five typical reshaping force-displacement curves of different two-steps clinched joints with different reshaping forces were shown in Fig. 3.2 using the same coordinate system with the same scale. The five reshaping force-displacement curves with different reshaping forces have high consistency in trend and shape.

As shown in Fig. 3.2, the whole reshaping process can be divided as two different stages by the changing rate of the reshaping force. The changing rate of the reshaping force is slower in the first stage. The plastic deformation occurred mainly on the protrusion of the conventional clinched joint. The changing rate of the reshaping force is faster in the second stage. The plastic deformation occurred simultaneously on the protrusion of the conventional clinched joint and the clinch-rivet. The plastic deformation of the clinch-rivet gave a rise to a rapid increase in the reshaping force.

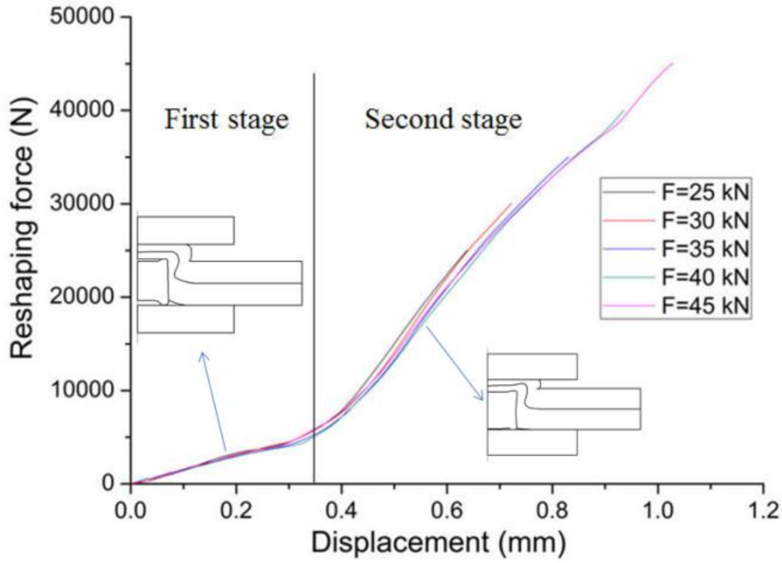

Fig. 3.2 The force-displacement curves of the reshaping process under different reshaping forces

3.1.2. Analysis of neck thickness and interlock

The interlock and neck thickness of the two-steps clinched joints with different reshaping forces are shown in Fig. 3.3. The interlock is increased with the increase of the reshaping force. The interlock of the joint with a reshaping force of 45 kN is the largest, while the neck thickness of the joint with a reshaping force of 35 kN is the largest. The interlock of the conventional clinched joint is 0.56 mm, while the neck thickness is 0.32 mm. The interlock and neck thickness of the conventional clinched joint are all smaller than those of the two-steps clinched joint.

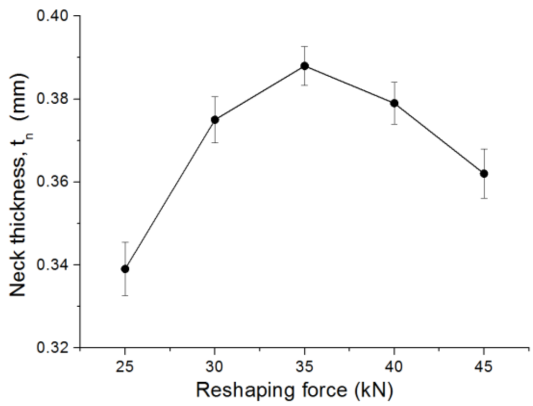

(a)

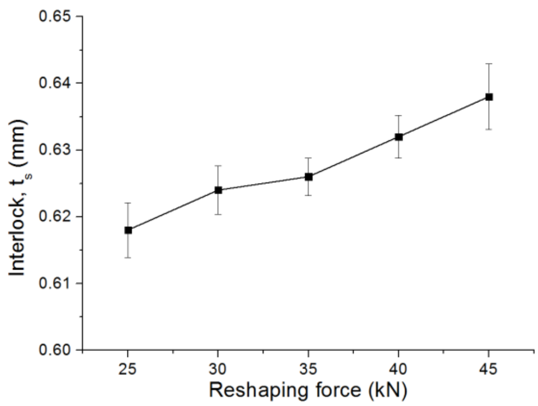

(b)

Fig. 3.3 Geometrical parameters of the two-steps clinched joint: (a) neck thickness; (b) interlock

3.2. Material flow

The cross-sectional profiles of the two-steps clinched joints with different reshaping forces are shown in Fig. 3.4. In order to make the comparison easily, the two-steps clinched joints with different reshaping forces and the conventional clinched joint are shown in the same figure. In the cross-sectional profile figures, the joints on the right side is the two-steps clinched joints with different reshaping forces, while the joints on the left side is the conventional clinched joints. The material around the upper pit and lower pit of the clinch-rivet can contribute to enlarge the interlock and neck thickness. The protrusion material will be compressed to flow downward under the reshaping force.

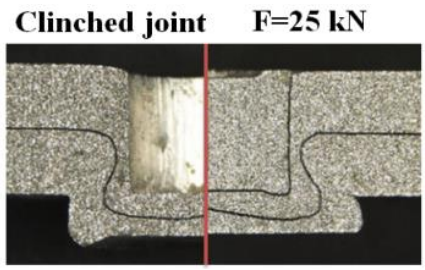

(a)

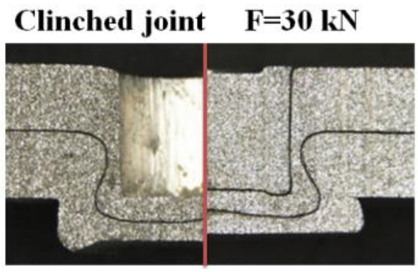

(b)

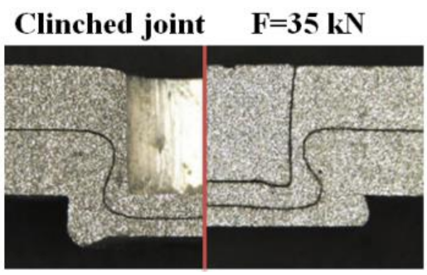

(c)

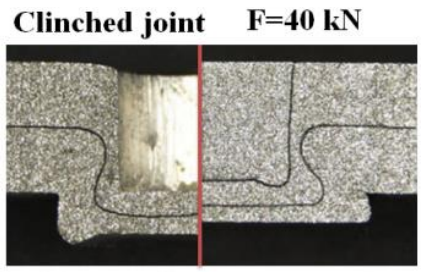

(d)

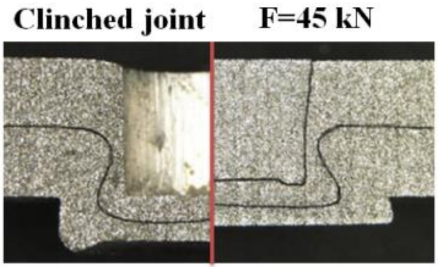

(e)

Fig. 3.4 Cross-sectional profiles of different clinched joints

The appearances of the protrusions on the conventional clinched joint and two-steps clinched joints with different reshaping forces are shown in Fig. 3.5.

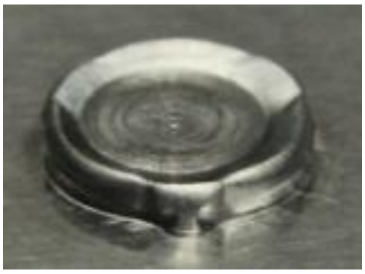

(a)

(b)

(c)

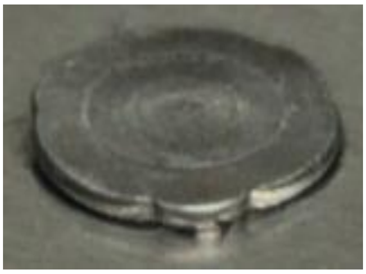

(d)

(e)

(f)

Fig. 3.5 Appearances of different clinched joints: (a)conventional clinched joint, (b) two-steps clinched joint with F=25 kN, (c) two-steps clinched joint with F=30 kN, (d) two-steps clinched joint with F=35 kN, (e) two-steps clinched joint with F=40 kN, (f) two-steps clinched joint with F=45 kN

Extensible dies were used to produce the conventional clinched joints, and three sliding sectors were contained in the extensible dies. So the protrusion of the conventional clinched joint is rugged. The three sliding sectors could control the material flow, which gave rise to three projecting bumps on the protrusion of the conventional clinched joint along the radial direction. The appearance of the two-steps clinched joint becomes smooth by the reshaping process, and the protrusion height of the joint is reduced.

The protrusion heights reshaped by different reshaping forces are shown in Fig. 3.6. The increase of the reshaping force gave a rise to the decrease of the protrusion height of the two-steps clinched joint. The protrusion height of the two-steps clinched joint with a reshaping force of 45 kN is 0.82 mm, while the protrusion height of the conventional clinched joint is 1.6 mm. The protrusion height of the two-steps clinched joint can be reduced significantly.

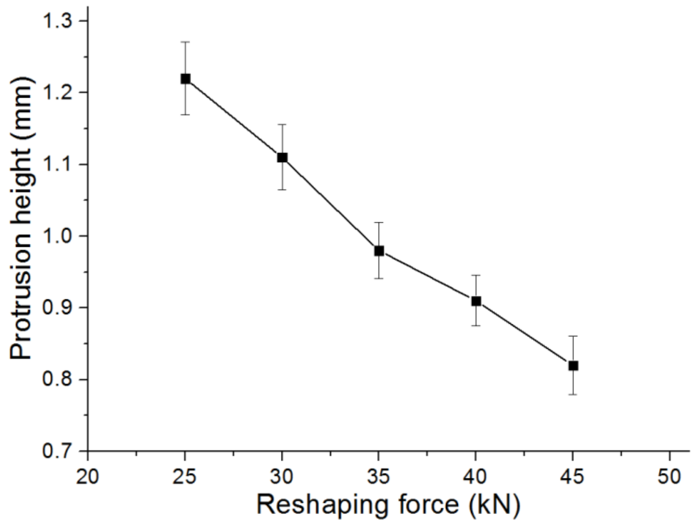

Fig. 3.6 Protrusion heights of the two-steps clinched joints

3.3. Mechanical behaviour

3.3.1. Static cross-tensile tests

The cross-tensile strengths of the two-steps clinched joints with different reshaping forces are shown in Fig. 3.7. The average cross-tensile strength of the two-steps clinched joints with a reshaping force of 35 kN is the highest, while the average cross-tensile strength of the conventional clinched joints is the lowest. The average cross-tensile strength of the two-steps clinched joints with a reshaping force of 35 kN is 1182 N, while the average cross-tensile strength of the conventional clinched joints is 948 N. Compared with the conventional clinched joints, the average cross-tensile strength of the two-steps clinched joints with a reshaping force of 35kN is increased by 25%. In the case of the reshaping forces of 25, 30, 35, 40 and 45 kN, the maximum cross-tensile strength can be gotten with the reshaping force of 35 kN.

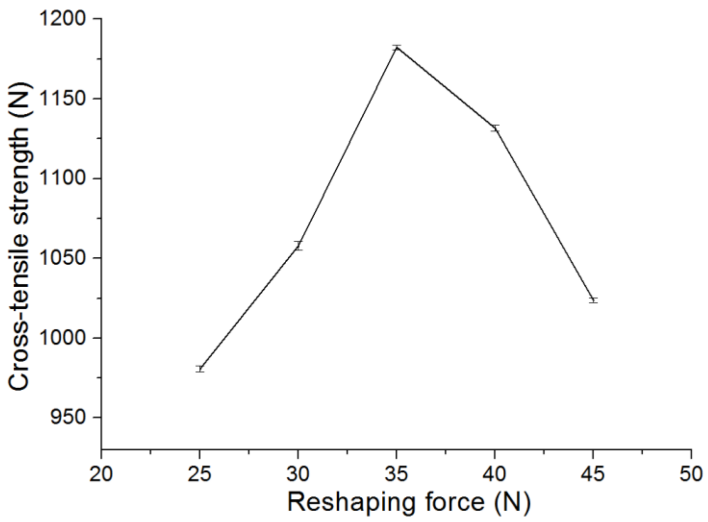

Fig. 3.7 Cross-tensile strengths of the two-steps clinched joints

In order to compare the cross-tensile strength easily, the typical cross-tensile force-displacement curves of the conventional clinched joint and different two-steps clinched joints are shown in Fig. 3.8. The two-steps clinched joints with different reshaping forces can undergo larger displacements before failure in the cross-tensile tests. For all the two-steps clinched joints in the cross-tensile tests, the cross-tensile force suddenly drops after the peak.

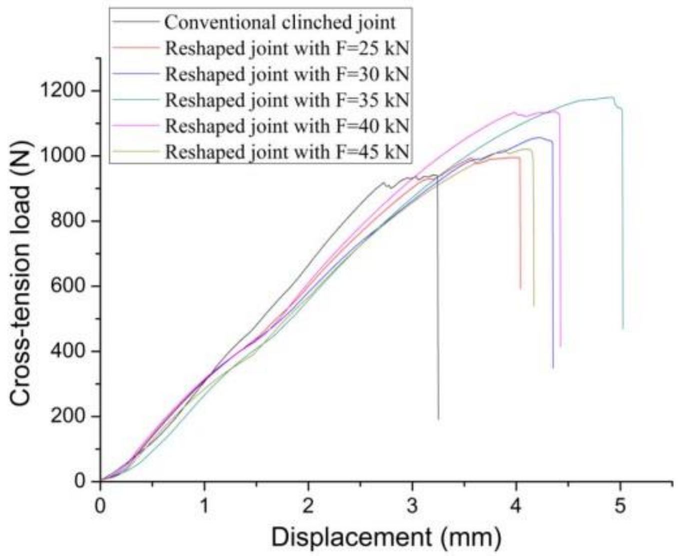

Fig. 3.8 Cross-tensile load-displacement curves of different joints

Neck fracture becomes the main failure mode for the two-steps clinched joint in the cross-tensile test as shown in Fig. 3.9. The neck thickness has an important influence on the joining strength of the two-steps clinched joint. A weak neck may generate the neck fracture mode. The cross-tensile strength has the same variation trend of the neck thickness. The cross-tensile strength can be increased by increasing the neck thickness. In order to get the joint with a higher strength, a thicker neck is required for the clinched joint.

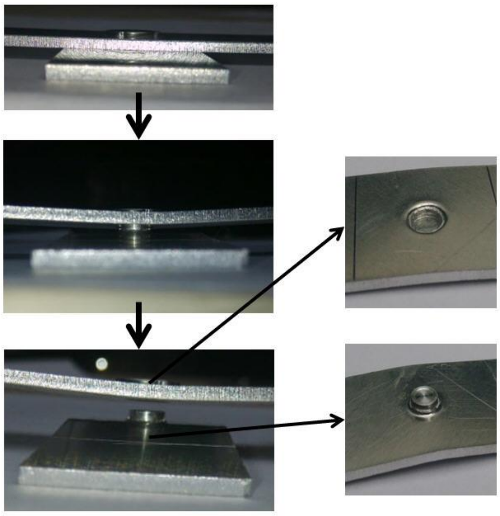

Fig. 3.9 Neck fracture mode of the two-steps clinched joint after the cross-tensile test

3.3.2. Static tension-shearing tests

The tension-shearing strengths of the two-steps clinched joints with different reshaping forces are shown in Fig. 3.10.

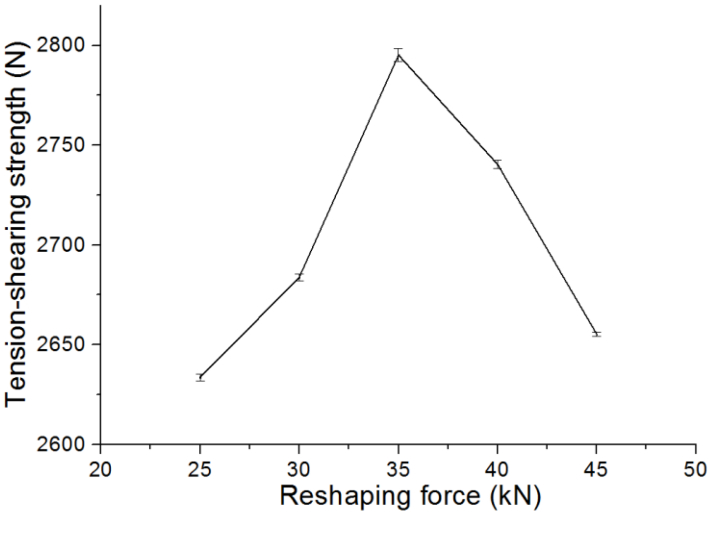

Fig. 3.10 Tension-shearing strengths of the two-steps clinched joints

The average tension-shearing strength of the two-steps clinched joints with a reshaping force of 35 kN is the highest, while the average tension-shearing strength of the conventional clinched joints is the lowest. The average tension-shearing strength of the two-steps clinched joint with a reshaping force of 35 kN is 2795 N, while the average tension-shearing strength of the clinched joints is 1225 N. Compared with the conventional clinched joints, the average tension-shearing strength of the two-steps clinched joints with a reshaping force of 35kN is increased by 128%.

The typical tension-shearing force-displacement curves of different joints are shown in Fig. 3.11. The two-steps clinched joints with different reshaping forces can undergo large displacements before failure in the tension-shearing tests.

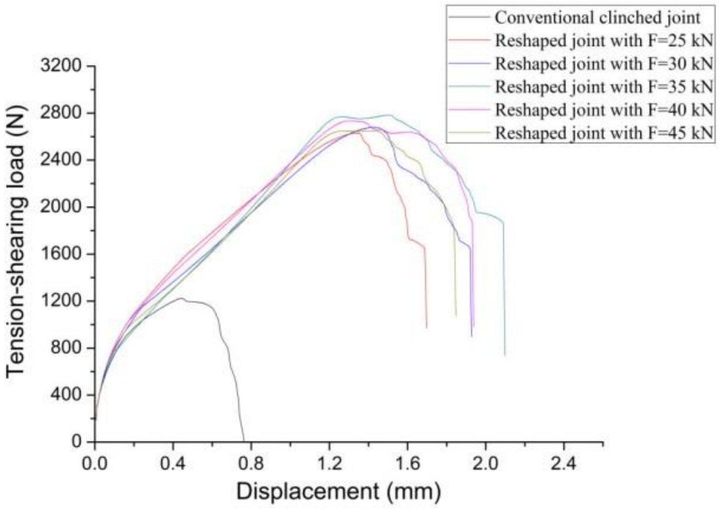

Fig. 3.11 Tension-shearing load-displacement curves of different joints

The average tension-shearing strength of the conventional clinched joints is 1.29 times higher than the average cross-tensile strength. The average tension-shearing strength of the two-steps clinched joints with a reshaping force of 35 kN is 2.36 times higher than the average cross-tensile strength. Compared with the cross-tensile strength, the two-steps clinching process can contribute to increase the tension-shearing strength effectively. The use of the clinch-rivet embedded in the two-steps clinched joint can help the clinched joint to bear the shearing force, which is effective to increase the tension-shearing strength.

Neck fracture is also the main failure mode for the two-steps clinched joint in the tension-shearing test as shown in Fig. 3.12. Neck thickness also has a great influence on the tension-shearing strength of the two-steps clinched joint. The two-steps clinching process can increase the tension-shearing strength by increasing the neck thickness.

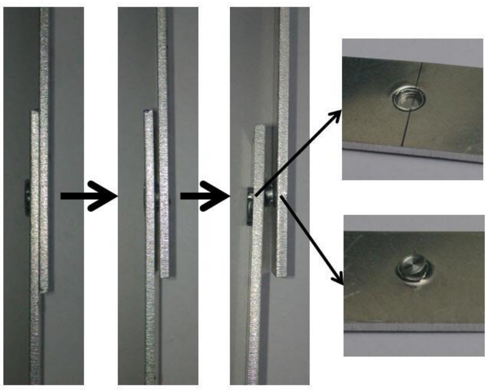

Fig. 3.12 Neck fracture mode of two-steps clinched joint after tension-shearing test

3.3.3. Energy absorption

The energy absorption of the conventional clinched joint and different two-steps clinched joints in the cross-tensile tests and tension-shearing tests are shown in Fig. 3.13. The energy absorption of the conventional clinched joint is the lowest, while the energy absorption of the two-steps clinched joint with a reshaping force of 35 kN is the highest of all. The energy absorption value of the two-steps clinched joint with a reshaping force of 35 kN is increased by 102% compared with the conventional clinched joint in the cross-tensile test. The energy absorption of two-steps clinched joint with a reshaping force of 35 kN is increased by 489% compared with the conventional clinched joint in the tension-shearing test.

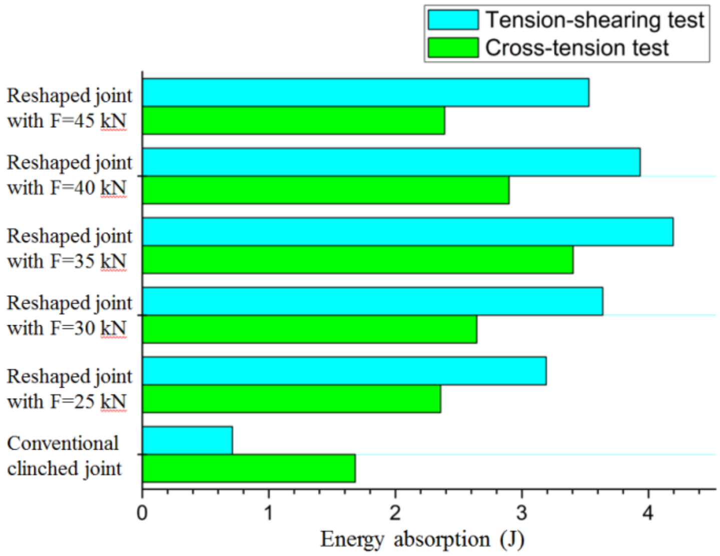

Fig. 3.13 Energy absorption of different joints

The energy absorption of conventional clinched joint in the tension-shearing test is lower than that in the cross-tensile test. However, the energy absorption values of two-steps clinched joint with different reshaping forces in the tension-shearing test are all higher than those in the cross-tensile test. The energy absorption of the two-steps clinched joint with a reshaping force of 35kN in the tension-shearing test is 23% higher than that in the cross-tensile test. The use of clinch-rivet can explain the phenomenon. The clinch-rivet used in the two-steps clinching process will deform to absorb more deformation energy in the tension-shearing test than that in the cross-tensile test.

3.4 Conclusions

The mechanical properties of the two-steps clinched joints were investigated in this chapter. The forming force and geometrical parameters of the two-steps clinched joint were obtained. Material flow of the two-steps clinched joint was studied to show the deformation process. The mechanical properties of the joint were also studied. The major conclusions of this chapter can be drawn as follows:

(1) Forming force is an important factor in the forming process. The neck thickness and interlock of the two-steps clinched joint are all larger than those of the clinched joint.

(2) The material flow in the reshaping process contributes to increase the strength and reduce the protrusion height of the clinched joint. The protrusion height of the two-steps clinched joint decreases with the increase of the reshaping force.

(3) The cross-tensile and tension-shearing strengths of the two-steps clinched joints with different reshaping forces are all higher than those of the conventional clinched joint. The cross-tensile and tension-shearing strengths of the two-steps clinched joint with a forming force of 35kN are the highest of all. Neck fracture mode is the main failure mode. Neck thickness has an important influence on the strength of the joint.

(4) The failure process of the two-steps clinched joint involves much higher energy absorption than the conventional clinched joint.

4 Effects of different parameters on the two-steps clinched joints

4.1 Two-steps clinching process for joining different aluminum alloy sheets

4.1.1 Materials

AL6061 and AL5052 were chosen as the sheet materials in the joining experiment for different aluminum alloy sheets. Rectangular AL5052 strips with 25 mm × 1.8 mm × 80 mm (width × thickness × length) were used in the experiment to carry out the two-steps clinching process, and rectangular AL6061 strips with 25 mm × 2 mm × 80 mm (width × thickness × length) were also used. In order to make the expression of the different mechanical clinched joints and two-steps clinched joints with different aluminum alloy sheets easily, the following terminologies to describe different joints are used:

MCAA6-5 joint: conventional mechanical clinched joint produced with AL6061 sheet (upper sheet) and AL5052 sheet (lower sheet);

MCAA5-6 joint: conventional mechanical clinched joint produced with AL5052 sheet (upper sheet) and AL6061 sheet (lower sheet);

TCAA6-5 joint: two-steps clinched joint produced with AL6061 sheet (upper sheet) and AL5052 sheet (lower sheet);

TCAA5-6 joint: two-steps clinched joint produced with AL5052 sheet (upper sheet) and AL6061 sheet (lower sheet).

4.1.2 Cross-sectional profiles of the joints with different aluminum alloy sheets

The cross-sectional profiles of the mechanical clinched joints and two-steps clinched joints with different aluminum alloy sheets are shown in Fig. 4.1. The clinched joints and the two-steps clinched joints are shown in the same figure. The left part of the figure is the two-steps clinched joint, and the right part of the figure is the conventional mechanical clinched joint. As can be seen, the neck thickness of the two-steps clinched joint is larger than that of the conventional mechanical clinched joint.

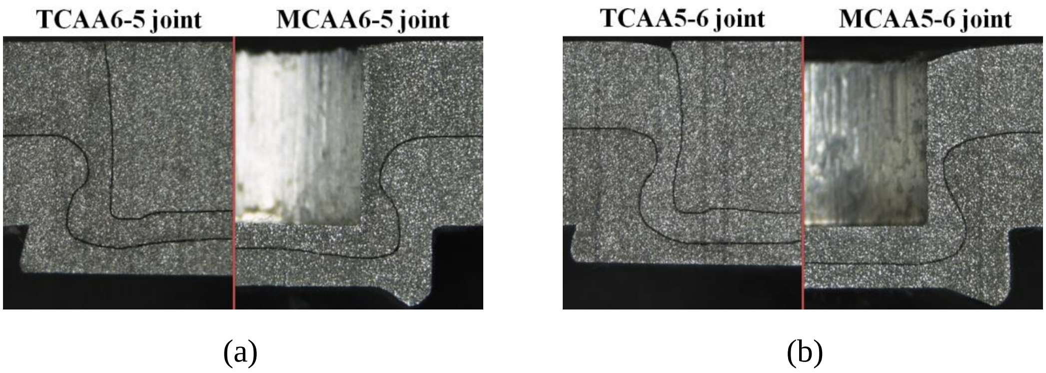

Fig. 4.1 Cross-sectional profiles of the joints: (a) TCAA6-5 joint and MCAA6-5 joint; (b) TCAA5-6 joint and MCAA5-6 joint

4.1.3 Mechanical properties of the joints with different aluminum alloy sheets

Cross-tensile tests were used to get the cross-tensile strengths of the different joints with different aluminum alloy sheets. Five specimens were used to get the average strength of the joint. The cross-tensile strengths of the different joints with different aluminum alloy sheets are shown in Fig. 4.2.

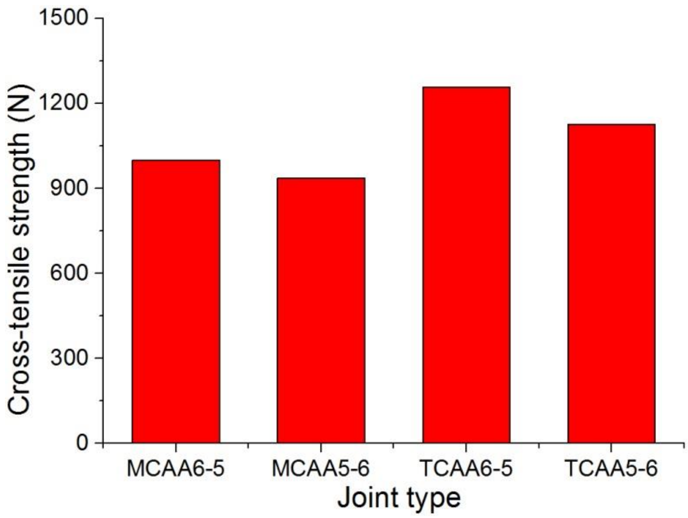

Fig. 4.2 Cross-tensile strengths of different joints

As can be seen, compared with other clinched joints, the MCAA5-6 joint has the lowest average cross-tensile strength, while the TCAA6-5 joint has the highest average cross-tensile strength. The TCAA6-5 joint has a higher average cross-tensile strength than the TCAA5-6 joint, and the MCAA6-5 joint has a higher average cross-tensile strength than the MCAA5-6 joint. The result proves that the joint with an upper sheet of AL6061 and a lower sheet of AL5052 has a higher cross-tensile strength than the joint with an upper sheet of AL5052 and a lower sheet of AL6061. It is necessary to take the AL6061 sheet as the upper sheet and AL5052 sheet as the lower sheet to get a higher cross-tensile strength in the joining of AL6061 sheet and AL5052 sheet.

The cross-tensile strength of the joint after reshaping process was increased. The cross-tensile strength of the TCAA6-5 joint is increased by 25.7% than that of the MCAA6-5 joint, and the cross-tensile of the TCAA5-6 joint is increased by 20.1% than that of the MCAA5-6 joint. This proves that the reshaping method in the second step is helpful to increase the cross-tensile strength for the joints with different aluminum alloy sheets. The reshaping method not only can reduce the protrusion height of the clinched joint, but also can increase the cross-tensile strength. The rivet placed in the pit can contribute to increase the cross-tensile of the joint.

The cross-tensile force-displacement curves of the joints with different sheets are shown in Fig. 4.3. All the force-displacement curves keep rising before the maximum force peak. The cross-tensile force-displacement curve drops at once after the maximum force peak. The cross-tensile force-displacement curves of the two-steps clinched joints after the reshaping process undergo larger displacement than those curves of the conventional mechanical clinched joint. The reshaping method used in the second step can be used to enlarge the displacement of the clinched joint before failure, which is significant for building the structure of the automobile.

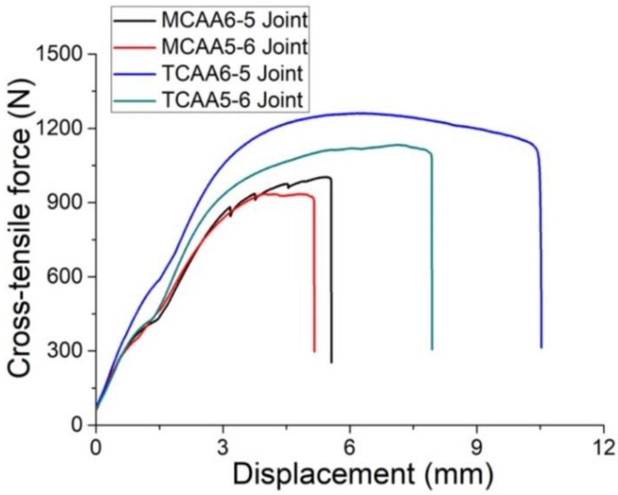

Fig. 4.3 Cross-tensile force-displacement curves

The energy absorption of the clinched joint is one of the important factors for evaluating the shocking resistance of the automotive structure. In order to increase the energy absorption, more energy must be absorbed by the joint before the failure. The value of energy absorption in the failing process was gotten by measuring the area between the force-displacement curve and the abscissa in the coordinate system. The energy absorption of the different joints with different sheets in the cross-tensile tests is shown in Fig. 4.4.

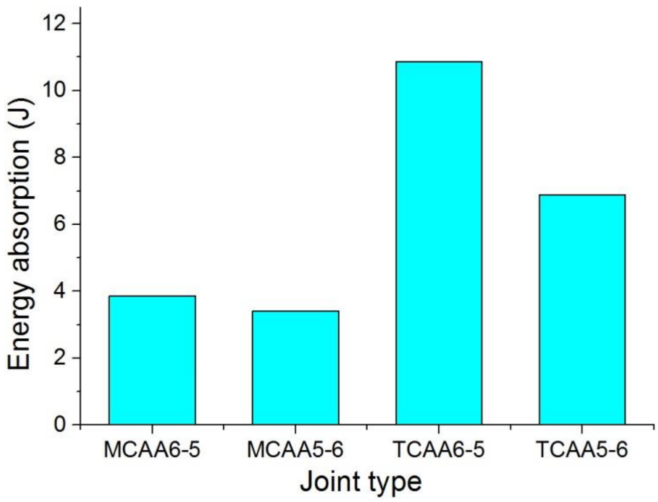

Fig. 4.4 Energy absorption in the cross-tensile test

The energy absorption of the MCAA5-6 joint is the lowest, while the energy absorption of the TCAA6-5 joint is the highest. The TCAA6-5 joint has higher energy absorption than the MCAA6-5 joint in the cross-tensile test, and the TCAA5-6 joint has higher energy absorption than the MCAA5-6 joint. This proves that the energy absorption of the joint after reshaping process in the second step can be increased by the reshaping process. The TCAA6-5 joint has higher energy absorption than the TCAA5-6 joint in the cross-tensile test, and the MCAA6-5 joint has higher energy absorption than the MCAA5-6 joint. The result proves that the joint with an upper sheet of AL6061 and a lower sheet of AL5052 has higher energy absorption in the cross-tensile test than the joint with an upper sheet of AL5052 and a lower sheet of AL6061.

Tension-shearing tests were used to get the tension-shearing strengths of the different joints with different aluminum alloy sheets. Five specimens were used to get the average strength of the joint. The tension-shearing strengths of the different joints with different aluminum alloy sheets are shown in Fig. 4.5.

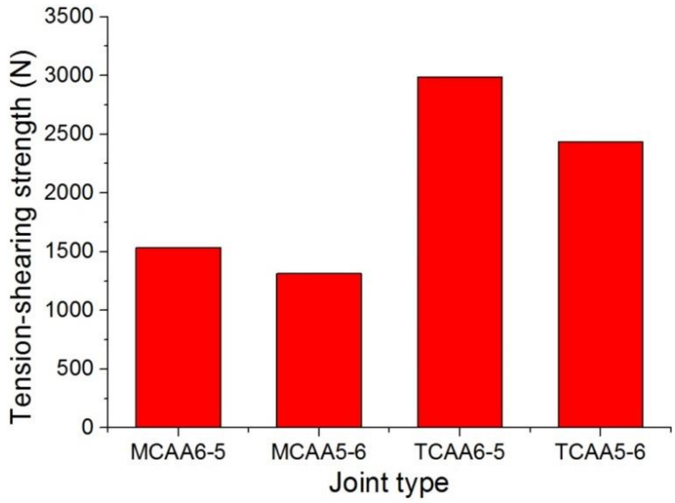

Fig. 4.5 Tension-shearing strengths of different joints

The tension-shearing strengths of the joints are all larger than the cross-tensile strength. Compared with other joints, the MCAA5-6 joint has the lowest average tension-shearing strength, while the TCAA6-5 joint has the highest average tension-shearing strength. The TCAA6-5 joint has a higher average tension-shearing strength than the TCAA5-6 joint, and the MCAA6-5 joint has a higher average tension-shearing strength than the MCAA5-6 joint. The result proves that the joint with an upper sheet of AL6061 and a lower sheet of AL5052 has a higher tension-shearing strength than the joint with an upper sheet of AL5052 and a lower sheet of AL6061. In the joining of AL6061 sheet and AL5052 sheet, the AL6061 sheet has better to be taken as the upper sheet and the AL5052 sheet has better to be taken as the lower sheet to get a higher tension-shearing strength.

The tension-shearing strength of the joint after reshaping process was increased. The tension-shearing of the TCAA6-5 joint is increased by 94.3% than that of the MCAA6-5 joint, and the tension-shearing of the TCAA5-6 joint is increased by 85.6% than that of the MCAA5-6 joint. This proves that the reshaping method is helpful for the joint to increase the tension-shearing strength. The rivet can help the joint to bear the shearing load in the tension-shearing test, so the strength of joint is increased a lot after the reshaping process.

The tension-shearing force-displacement curves of the joints with different sheets are shown in Fig. 4.6. The variation trend of the tension-shearing force-displacement curve is different with that of the cross-tensile force-displacement curve. All the force-displacement curves keep rising before the maximum force peak. The tension-shearing force-displacement curve drops gradually after the maximum force peak. The tension-shearing force-displacement curves of the joints after the reshaping process undergo larger displacement than those curves of the clinched joint before the reshaping process.

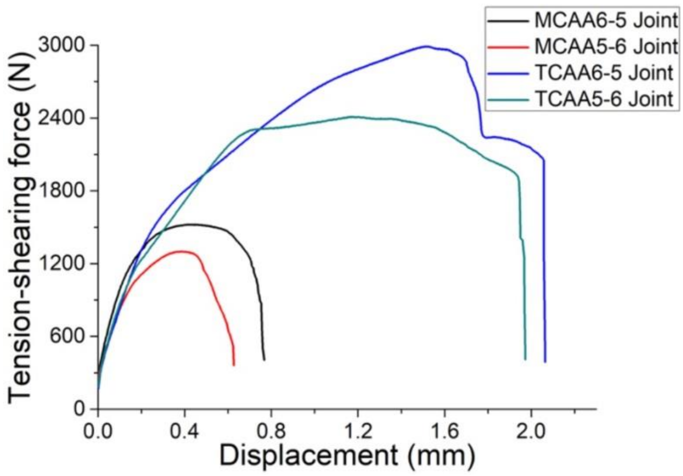

Fig. 4.6 Tension-shearing force-displacement curves

The energy absorption of different joints with different aluminum alloy sheets in the tension-shearing test is shown in Fig. 4.7.

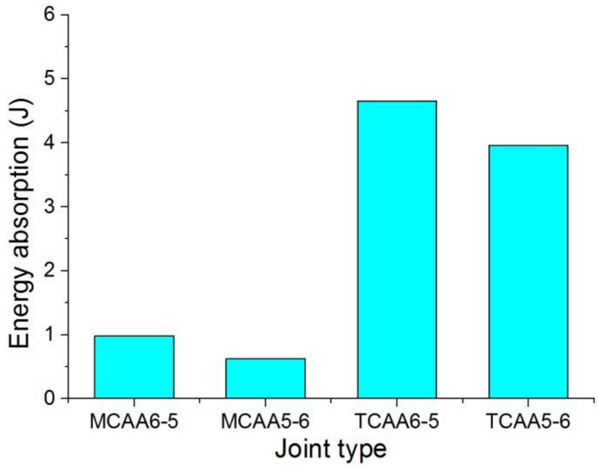

Fig. 4.7 Energy absorption in the tension-shearing test

The relative magnitude of the energy absorption in tension-shearing test is similar with that in the cross-tensile test. The energy absorption of the MCAA5-6 joint in tension-shearing test is the lowest, while the energy absorption of the TCAA6-5 joint is the highest. The TCAA6-5 joint has higher energy absorption than the MCAA6-5 joint in the tension-shearing test, and the TCAA5-6 joint has higher energy absorption than the MCAA5-6 joint. This proves that the energy absorption of the joint after reshaping process can be increased by the reshaping process. The TCAA6-5 joint has higher energy absorption than the TCAA5-6 joint in the tension-shearing test, and the MCAA6-5 joint has higher energy absorption than the MCAA5-6 joint. The result proves that the joint with an upper sheet of AL6061 and a lower sheet of AL5052 has higher energy absorption in the tension-shearing test than the joint with an upper sheet of AL5052 and a lower sheet of AL6061.

4.2 Two-steps clinching process for joining aluminum alloy sheets with different thicknesses

4.2.1 Aluminum alloy sheets with different thicknesses

In order to investigate the influence of different sheet thicknesses on the mechanical properties of the clinched joint, Al5052 aluminum alloy sheets with thicknesses of 2.0 mm and 2.5 mm were used to produce the clinched joint in this study. In order to make the description of the joints with different sheet thicknesses easily, the following terminologies are used in this paper:

CLJ2.5-2.0 joint: conventional clinched joint produced by the sheet with a thickness of 2.0 mm (lower sheet) and the sheet with a thickness of 2.5 mm (upper sheet);

CLJ2.0-2.5 joint: conventional clinched joint produced by the sheet with a thickness of 2.5 mm (lower sheet) and the sheet with a thickness of 2.0 mm (upper sheet);

COJ2.5-2.0 joint: two-steps clinched joint produced by the sheet with a thickness of 2.0 mm (lower sheet) and the sheet with a thickness of 2.5 mm (upper sheet);

COJ2.0-2.5 joint: two-steps clinched joint produced by the sheet with a thickness of 2.5 mm (lower sheet) and the sheet with a thickness of 2.0 mm (upper sheet).

4.2.2 Cross-sectional profiles of the joints with different sheet thicknesses

An interlock was produced in the clinching process to hook the sheets together. The feasibility of the reshaping process can be guaranteed by investigating whether the interlock is damaged or not in the reshaping process. The cross-sectional profiles of the conventional mechanical clinched joint and two-steps clinched joint are shown in Fig. 4.8. In order to compare the two-steps clinched joint with the conventional clinched joint easily, the two different joints are shown in the same figure. The joint on the left half side of the figure is conventional mechanical clinched joint (before reshaping), and the joint on the right half side of the figure is two-steps clinched joint (after reshaping).

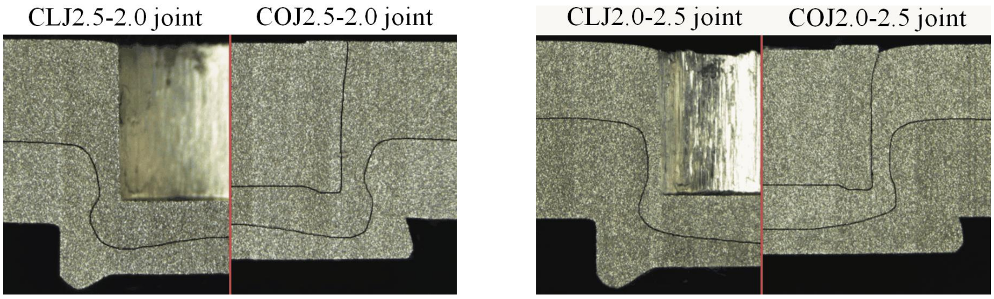

(a) (b)

Fig. 4.8 Cross-sectional profiles of the joints: (a) CLJ2.5-2.0 joint and COJ2.5-2.0 joint; (b) CLJ2.0-2.5 joint and COJ2.0-2.5 joint

As can be seen from the figures, the mechanical interlock of the clinched joint is not damaged in the reshaping process. The sheets are still hooked together by the mechanical interlock. The neck area of the joint is strengthened by the reshaping process in the second step. After the reshaping process, the protrusion height of the clinched joint is reduced. With a lower protrusion, the two-steps clinched joint can be used in the visible areas.

4.2.3 Mechanical properties of the joints with different sheet thicknesses

The cross-tensile strength and tension-shearing strength are two main strength types for the clinched joint. It is better for the two-steps clinched joint to have a higher strength.

The cross-tensile strengths of the conventional mechanical clinched joints and two-steps clinched joints with different sheet thicknesses are shown in Fig. 4.9. The COJ2.5-2.0 joint has the highest cross-tensile strength, while the CLJ2.0-2.5 joint has the lowest cross-tensile strength.

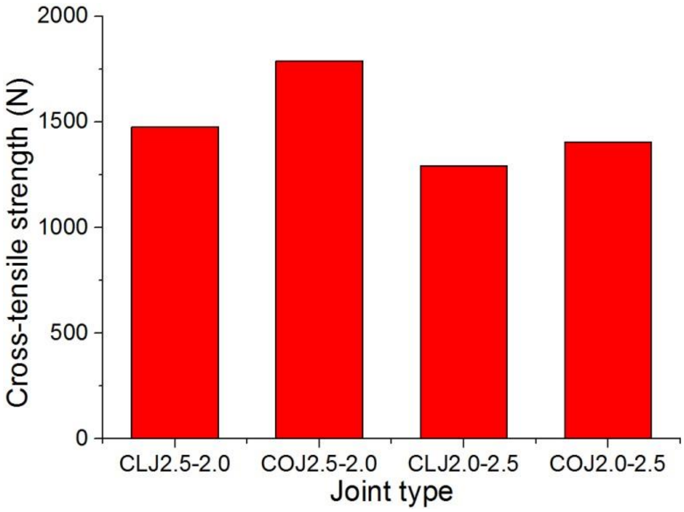

Fig. 4.9 Cross-tensile strengths of the joints

The cross-tensile strength of the COJ2.5-2.0 joint is 21.1% higher than that of the CLJ2.5-2.0 joint, and the cross-tensile strength of the COJ2.0-2.5 joint is 8.7% higher than that of the CLJ2.0-2.5 joint. The two-steps clinched joint has higher cross-tensile strength than the conventional mechanical clinched joint, which proves that the reshaping process in the second step can result in higher cross-tensile strength for joining sheets with different thicknesses.

The increase in cross-tensile strength of the two-steps clinched joint was caused by the rivet and the increased neck thickness. The two-steps clinching process can increase the strength of the joint by increasing the neck thickness. In addition, the rivet embedded in the pit of the joint also can help the two-steps clinched joint to increase the strength. The rivet is kept in the pit of the joint after the reshaping process, which also can help the joint to bear the tensile load. So the two-steps clinched joint has higher tensile strength than the clinched joint.

The reshaping process in the second step also influences the stiffness of the joint.

When the rivet is used, the cavity formed by the punch is fulfilled; thus, the stiffness of the joint can be increased by the rivet, which also contributes to increase the strength of the joint.

The cross-tensile strength of the CLJ2.5-2.0 joint is 14.4% higher than that of the CLJ2.0-2.5 joint, and the cross-tensile strength of the COJ2.5-2.0 joint is 27.5% higher than that of the COJ2.0-2.5 joint. The joint with a thick upper sheet has higher cross-tensile strength than the joint with a thin upper sheet. The thick upper sheet results in a large neck thickness, which can help the joint to get higher cross-tensile strength.

The typical cross-tensile force-displacement curves of the joints are shown in Fig. 4.10. All the cross-tensile force-displacement curves of the joints have the similar development trend. Before the force peak, the cross-tensile forces were increased with the increase of the displacement. After the force peak, the cross-tensile force-displacement curves dropped rapidly. The two-steps clinched joint has a longer displacement than the conventional clinched joint before failure, and the joint with a thicker upper sheet also has a longer displacement than the joint with a thinner upper sheet.

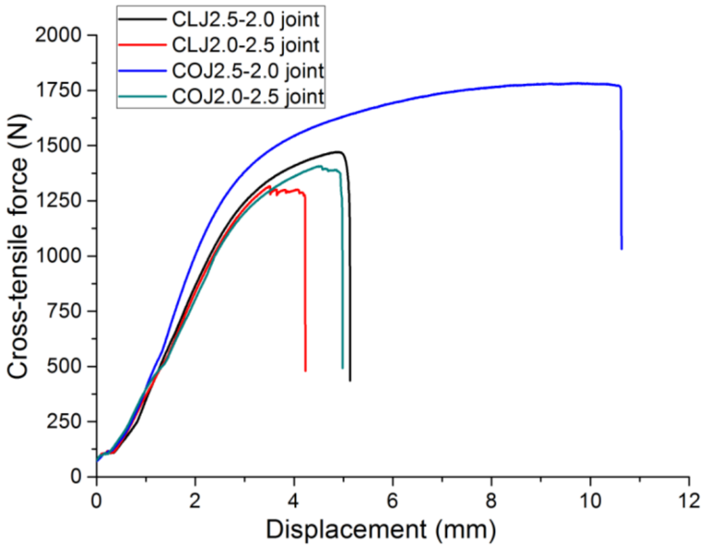

Fig. 4.10 Cross-tensile force-displacement curves

Higher energy absorption of the joint means higher safety of the automotive body. The energy absorption of the joints with different sheet thicknesses in the cross-tensile test is shown in Fig. 4.11.

The COJ2.5-2.0 joint has higher energy absorption than the CLJ2.5-2.0 joint in the cross-tensile test, and the COJ2.0-2.5 joint has higher energy absorption than the CLJ2.0-2.5 joint. The two-steps clinched joint has higher energy absorption than the conventional clinched joint in the cross-tensile test, which proves that the reshaping process in the second step can contribute to increase the energy absorption of the clinched joint in the cross-tensile test. The neck thickness is enlarged in the reshaping process, which can help the clinched joint to increase the energy absorption. In addition, the rivet embedded in the pit of the joint also can help the two-steps clinched joint to increase the energy absorption. The rivet will deform to absorb more energy, which contributes to guarantee the safety of the joint.

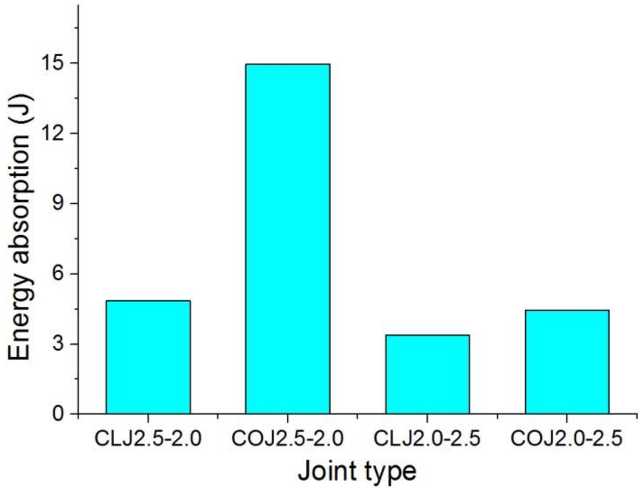

Fig. 4.11 Energy absorption in the cross-tensile test

The CLJ2.5-2.0 joint has higher energy absorption than the CLJ2.0-2.5 joint in the cross-tensile test, and the COJ2.5-2.0 joint has higher energy absorption than the COJ2.0-2.5 joint. The joint with a thick upper sheet has higher energy absorption than the joint with a thin upper sheet in the cross-tensile test. The thick upper sheet results in a large neck thickness, which contributes to increase the energy absorption of the joint in the cross-tensile test.

The tension-shearing strengths of the clinched joints and two-steps clinched joints are shown in Fig. 4.12. The COJ2.5-2.0 joint has the highest tension-shearing strength, while the CLJ2.0-2.5 joint has the lowest tension-shearing strength.

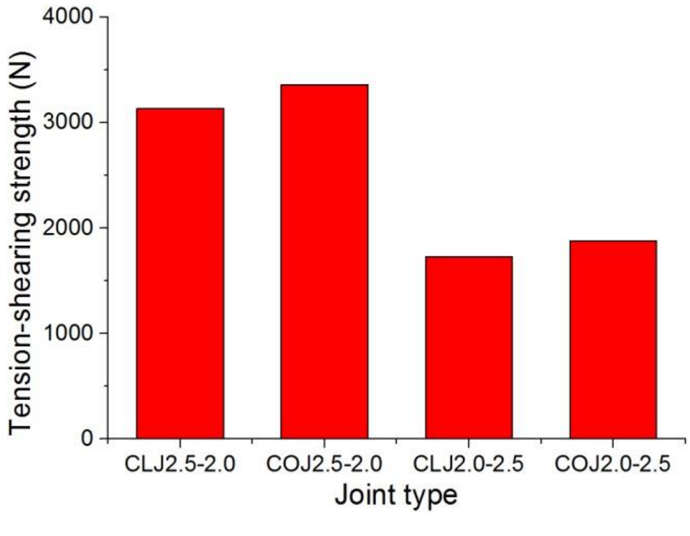

Fig. 4.12 Tension-shearing strengths of the joints

The tension-shearing strength of the COJ2.5-2.0 joint is 7.1% higher than that of the CLJ2.5-2.0 joint, and the tension-shearing strength of the COJ2.0-2.5 joint is 8.4% higher than that of the CLJ2.0-2.5 joint. The two-steps clinched joint has higher tension-shearing strength than the conventional clinched joint, which proves that the reshaping process in the second step can result in higher tension-shearing strength.

The rivet embedded in the pit of the joint can help the two-steps clinched joint to increase the strength. The rivet is kept in the pit of the joint after the reshaping process, which also can help the joint to bear the shearing load. So the two-steps clinched joint has higher tension-shearing strength than the conventional clinched joint.

The tension-shearing strength of the CLJ2.5-2.0 joint is 81.1% higher than that of the CLJ2.0-2.5 joint, and the tension-shearing strength of the COJ2.5-2.0 joint is 79.1% higher than that of the COJ2.0-2.5 joint. The joint with a thick upper sheet has higher tension-shearing strength than the joint with a thin upper sheet. The thick upper sheet results in a large neck thickness, which can help the joint to get a higher tension-shearing strength.

The typical tension-shearing force-displacement curves of the joints are shown in Fig. 4.13. As for the tension-shearing force-displacement curve, before the force peak, the tension-shearing forces were increased with the increase of the displacement. After the force peak, the tension-shearing force-displacement curves dropped gradually. The two-steps clinched joint has a longer displacement than the conventional clinched joint before failure, and the joint with a thick upper sheet also has a longer displacement than the joint with a thin upper sheet.

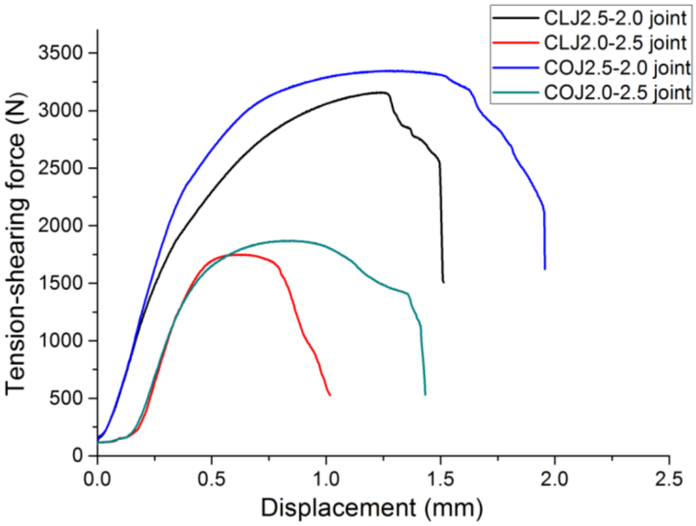

Fig. 4.13 Tension-shearing force-displacement curves

The energy absorption of the joints with different sheet thicknesses in the tension-shearing test is shown in Fig. 4.14.

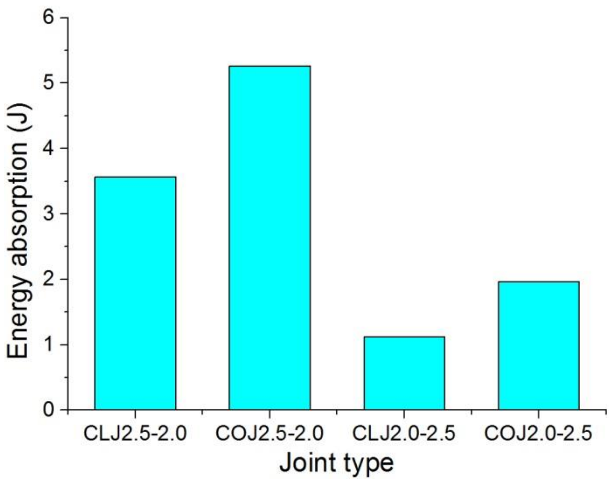

Fig. 4.14 Energy absorption in the tension-shearing test

The COJ2.5-2.0 joint has higher energy absorption than the CLJ2.5-2.0 joint in the tension-shearing test, and the COJ2.0-2.5 joint has higher energy absorption than the CLJ2.0-2.5 joint. The two-steps clinched joint has higher energy absorption than the conventional clinched joint, which proves that the reshaping process in the second step can contribute to increase the energy absorption of the clinched joint in the tension-shearing test.

The CLJ2.5-2.0 joint has higher energy absorption than the CLJ2.0-2.5 joint in the tension-shearing test, and the COJ2.5-2.0 joint has higher energy absorption than the COJ2.0-2.5 joint. The joint with a thick upper sheet has higher energy absorption than the joint with a thin upper sheet in the tension-shearing test. The thick upper sheet results in a large neck thickness, which contributes to increase the energy absorption of the joint in the tension-shearing test.

4.3 Two-steps clinched joint with different geometrical parameters

4.3.1 Material and joints with different geometrical parameters

AL5052 sheet was used to investigate two-steps clinching process for joining aluminum alloy sheets with different geometrical parameters. The main geometrical parameters of the clinched joint are neck thickness, interlock and bottom thickness. The neck thickness and interlock are difficult to measure without cutting the joint along the center shaft. The bottom thickness (X) is easy to measure without damage to the clinched joint. So the bottom thickness is always taken as the main measuring parameter to evaluate the quality of the clinched joint. The clinched joints were produced with bottom thicknesses of 1.4, 1.5, and1.6 mm respectively by controlling the punch displacement. In order to make the description of the joints with different sheet thicknesses easily, the following terminologies are used in this paper:

MCJ1.4 joint: conventional mechanical clinched joint with a bottom thickness of 1.4 mm;

MCJ1.5 joint: conventional mechanical clinched joint with a bottom thickness of 1.5 mm;

MCJ1.6 joint: conventional mechanical clinched joint with a bottom thickness of 1.6 mm;

TCJ1.4 joint: two-steps clinched joint with a bottom thickness of 1.4 mm;

TCJ1.5 joint: two-steps clinched joint with a bottom thickness of 1.5 mm;

TCJ1.6 joint: two-steps clinched joint with a bottom thickness of 1.6 mm.

4.3.2 Cross-sectional profiles of the joints with different geometrical parameters

The comparison of the appearances and cross-sectional profiles of the two-steps clinched joint with a bottom thickness of 1.4 mm and the conventional mechanical clinched joint with a bottom thickness of 1.4 mm are shown in Fig. 4.15. The left part of the figure is the two-steps clinched joint with a bottom thickness of 1.4 mm, and the right part of the figure is the conventional mechanical clinched joint with a bottom thickness of 1.4 mm. As can be seen, the upper sheet and lower sheet are still hooked together by the interlock after the reshaping process. The neck thickness was increased by reshaping the protrusion, and the protrusion height was reduced.

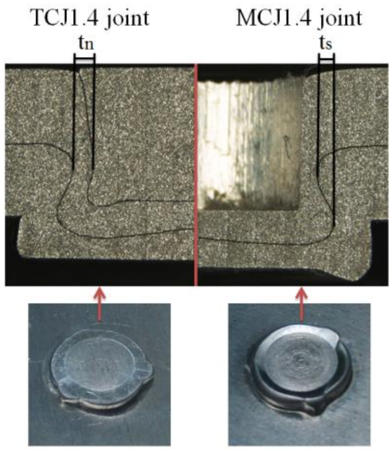

Fig. 4.15 Appearances and cross-sectional shapes of the joints

4.3.3 Mechanical properties of the joints with different geometrical parameters

The cross-tensile strengths of the conventional clinched joints and two-steps clinched joints with different geometrical parameters are shown in Fig. 4.16. The bottom thickness was taken as the variable parameter. Five samples were tested for each strength test to get the average cross-tensile strength of the joint.

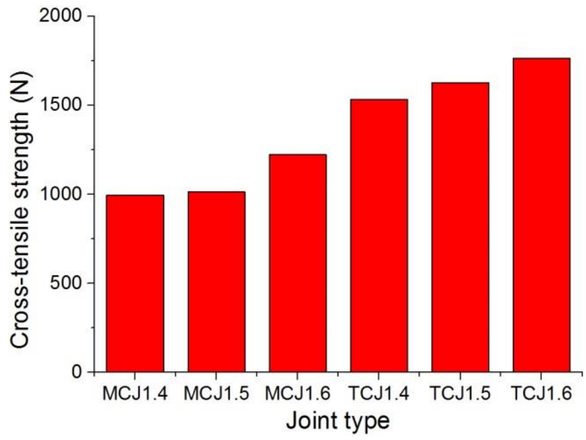

Fig. 4.16 Cross-tensile strengths of the joints

All of the conventional clinched joints with different geometrical parameters have lower cross-tensile strengths than the two-steps clinched joints. The cross-tensile strength of the joint can be increased by the reshaping method. The two-steps clinched joint with a bottom thickness of 1.6 mm has the highest cross-tensile strength among all the joints, and the conventional clinched joint with a bottom thickness of 1.4 mm has the lowest cross-tensile strength. The cross-tensile strength of the two-steps clinched joint with a bottom thickness of 1.6 mm was increased by 44.4% compared with that of the clinched joint with a bottom thickness of 1.6 mm.

The cross-tensile force-displacement curves of different joints with different geometrical parameters are shown in Fig. 4.17. The cross-tensile force-displacement curves have similar growing trend. The curves dropped at once after the force peak.

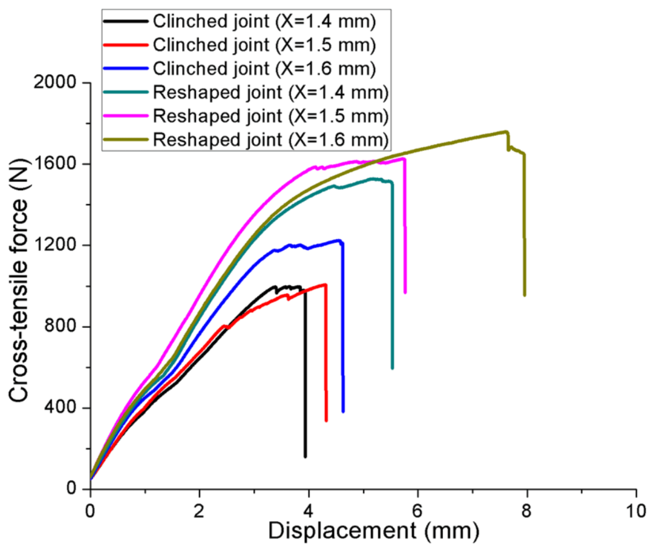

Fig. 4.17 Cross-tensile force-displacement curves

As for the joint used on the automotive body, a better performance for energy absorption is required. The energy absorption in the failure process is an important parameter to evaluate the quality of the joint. The energy absorption of different joints with different geometrical parameters in the cross-tensile tests is shown in Fig. 4.18.

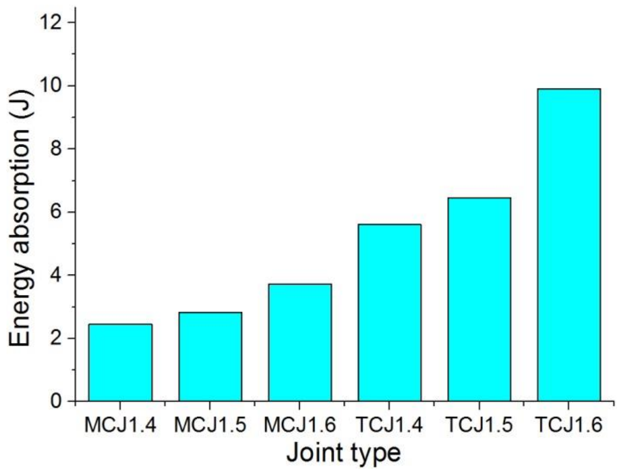

Fig. 4.18 Energy absorption in the cross-tensile test

As can be seen, the two-steps clinched joint with a bottom thickness of 1.6 mm has the highest energy absorption among two-steps clinched joints, and the clinched joint with a bottom thickness of 1.6 mm has the highest energy absorption strength among the clinched joints. The energy absorption of the two-steps clinched joint with a bottom thickness of 1.6 mm was increased by 165.9% compared with that of the clinched joint with a bottom thickness of 1.6 mm in the cross-tensile test. The reshaping method in the second step can help the joint to absorb more energy in the cross-tensile test. With higher energy absorption, the safety of the joining of aluminum alloy sheet on the automobile can be improved.

The tension-shearing strengths of the conventional clinched joints and two-steps clinched joints with different geometrical parameters are shown in Fig. 4.19.

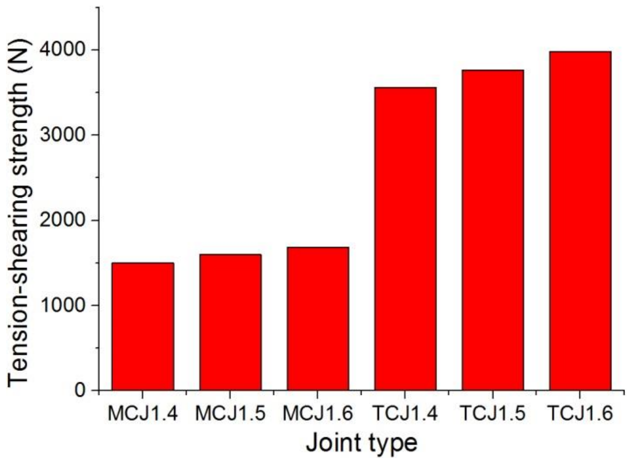

Fig. 4.19 Tension-shearing strengths of the joints

As can be seen, all of the conventional clinched joints with different geometrical parameters have lower tension-shearing strengths than the two-steps clinched joints with different geometrical parameters. The tension-shearing strength of the joint can be increased by the reshaping method.

The two-steps clinched joint with a bottom thickness of 1.6 mm has the highest tension-shearing strength among the two-steps clinched joints, and the clinched joint with a bottom thickness of 1.6 mm has the highest tension-shearing strength among the clinched joints. The tension-shearing strength of the two-steps clinched joint with a bottom thickness of 1.6 mm was increased by 136.5% compared with that of the clinched joint with a bottom thickness of 1.6 mm. The reshaping method is effective for increasing the tension-shearing strength of the joint.

The two-steps clinched joint showed larger tension–shearing strength due to the rivet. The rivet placed in the pit of the joint can help the joint to bear the tension-shearing load in the tension-shearing test. With the help of the rivet, the joint can bear a higher tension-shearing load.

The tension-shearing force-displacement curves of different joints with different geometrical parameters are shown in Fig. 4.20. As can be seen, the tension-shearing forces were increased with the increase of the displacements before the force peak. After the force peak, the joints were fractured, and the curves gradually dropped, which is different with the cross-tensile force-displacement curves. The two-steps clinched joints with different geometrical parameters have larger displacements than the clinched joints. This proves that the two-steps clinched joint has a better performance for resistance to failure than the conventional clinched joint.

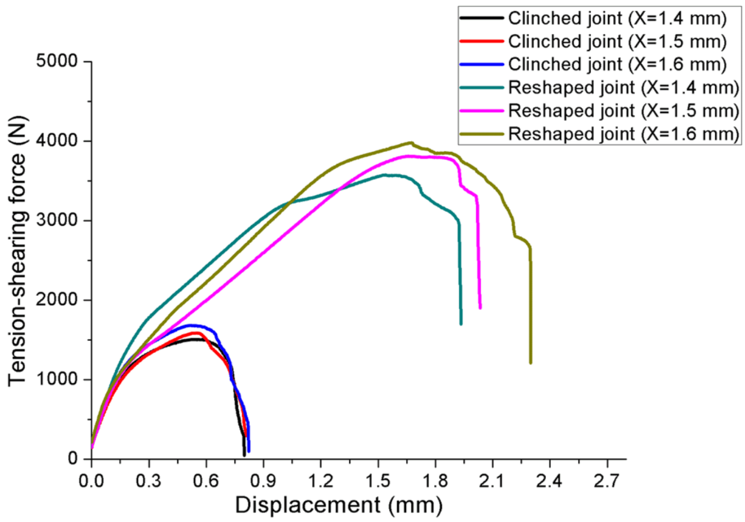

Fig. 4.20 Tension-shearing force-displacement curves

The energy absorption of different joints in the tension-shearing tests is shown in Fig. 4.21. As can be seen, the two-steps clinched joint with a bottom thickness of 1.6 mm has the highest energy absorption among the two-steps clinched joints, and the conventional clinched joint with a bottom thickness of 1.6 mm has the highest energy absorption strength among the conventional clinched joints. The energy absorption of the two-steps clinched joint with a bottom thickness of 1.6 mm was increased by 537.6% compared with that of the conventional clinched joint with a bottom thickness of 1.6 mm in the tension-shearing test. The reshaping process in the second step can help the joint to absorb more energy in the tension-shearing test.

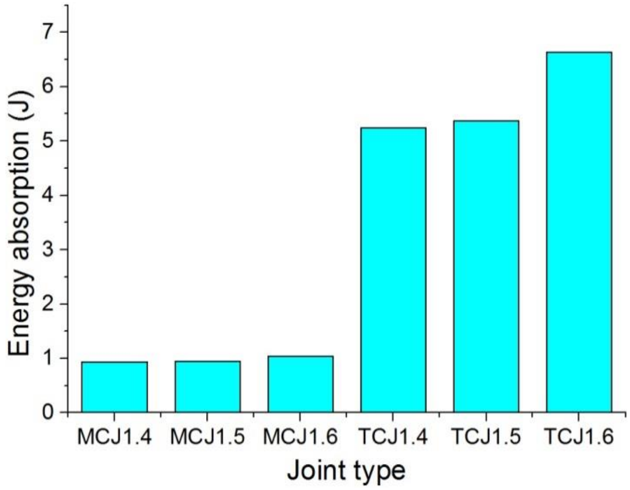

Fig. 4.21 Energy absorption in the tension-shearing test

4.4 Conclusion

The two-steps clinching process used for joining aluminum alloy sheets with different parameters was investigated in this chapter. Firstly, the two-steps clinching process was used to join different aluminum alloy sheets. Secondly, the two-steps clinching process was used to join aluminum alloy sheets with different thicknesses. At last, the two-steps clinched joints with different geometrical parameters were investigated by changing the bottom thickness. The major conclusions of this chapter can be drawn as follows:

(1) The two-steps clinching process is suitable for joining different aluminum alloy sheets. The joint with an upper sheet of AL6061 and a lower sheet of AL5052 has higher strength than the joint with an upper sheet of AL5052 and a lower sheet of AL6061. The rivet can help the joint to increase the strength in the two-steps clinching process.

(2) The two-steps clinching process is suitable for joining aluminum alloy sheets with different thicknesses. The COJ2.5-2.0 joint has the highest strength, while the CLJ2.0-2.5 joint has the lowest strength. For joining aluminum alloy sheets with different thicknesses, it is better to take the thicker sheet as the upper sheet to get a higher strength.

(3) The two-steps clinched joint with a bottom thickness of 1.6 mm has the highest cross-tensile strength and tension-shearing strength among the two-steps clinched joints in case of the joints with bottom thicknesses of 1.4, 1.5, and 1.6 mm.

5 Comparative investigations of three different reshaping methods

5.1 Reshaping mechanism

5.1.1 Reshaping process with a rivet

In order to increase the static strength of the clinched joint, the clinched joint can be reshaped with a rivet. The reshaping process with a rivet is shown in Fig. 5.1. Two flat dies are used in the reshaping process. A rivet is applied to support the clinched joint and control the material flow. After a rivet is placed in the pit of the clinched joint, the clinched joint is compressed by the top flat die. With the movement of the top flat die, the protrusion height of the joint is reduced.

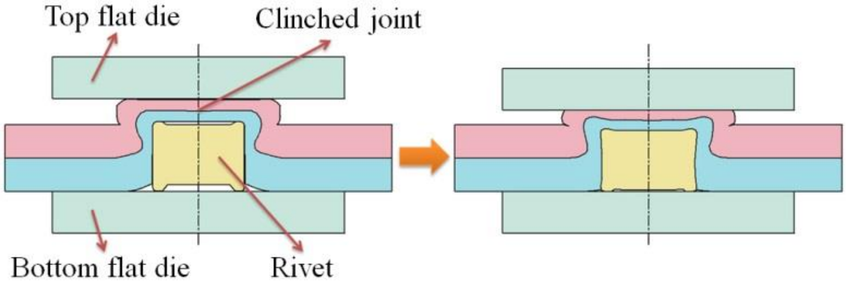

Fig. 5.1 The reshaping process with a rivet

5.1.2 Reshaping process with no auxiliary

The reshaping process with no auxiliary is shown in Fig. 5.2. The reshaping process with no auxiliary is similar with the reshaping process with a rivet. Two same flat dies are used to compress the clinched joint in both the two reshaping processes. The difference is that one reshaping process requires a rivet, and another process requires no rivet. With no rivet to support the joint, the clinched joint is compressed by the top flat die in a single stroke.

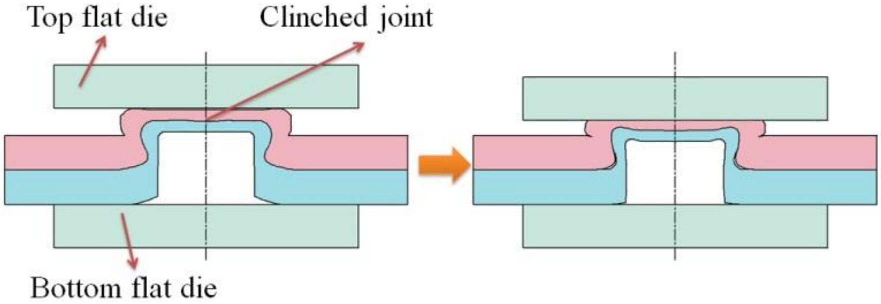

Fig. 5.2 The reshaping process with no auxiliary

5.1.3 Reshaping process with a bumped die

The reshaping process with a bumped die is shown in Fig. 5.3. A bumped die and a flat die are applied to reshape the joint. The bumped die is taken as the bottom die, and the flat die is taken as the top die. There is a bump for supporting the clinched joint on the bumped die. The bump can be placed in the pit of the clinched joint to control the material flow. The bumped die is fixed, and the top flat die can be controlled to move downward to compress the joint.

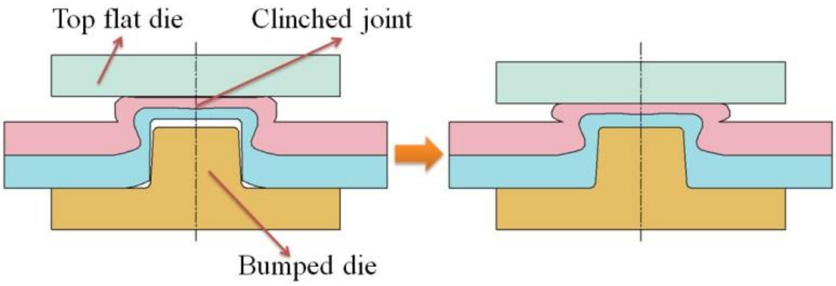

Fig. 5.3 The reshaping process with a bumped die

5.2 Material and experimental procedure

5.2.1 Material

Aluminum alloy AL6061 sheets have been widely applied to build the structure of the automotive body. AL6061 sheet has better formability, which is suitable for generating plastic deformation to produce the clinched joint.

In this study, AL6061-T4 was used as the material of the metal sheet. The mechanical properties of the AL6061-T4 sheet were measured on Instron 5982 tensile testing machine. The elastic modulus of the aluminum alloy AL6061-T4 is 66.5 GPa, tensile stress is 176 MPa, and poisson's ratio is 0.33.

All the AL6061-T4 sheets were cut from a large AL6061-T4 sheet (1200×2400 mm) along the rolling direction. The thickness of the AL6061-T4 sheet was 2 mm, which is widely used on the automotive body. The width of the sheet was 25 mm, and the length of the sheet was 80 mm.

5.2.2 Mechanical clinching process

Clinched joint was produced by plastic deformation in the mechanical clinching process. The process was conducted on a mechanical clinching machine produced by the express company. As shown in Fig. 5.4, extensible dies were used to produce the clinched joint. The extensible dies which were made of high strength steel consist of the anvil, punch, spring, sliding sectors and blank holder. The speed and displacement of the punch can be controlled precisely.

Fig. 5.4 Extensible dies

Two AL6061-T4 sheets were placed between the punch and sliding sectors. The punch moved downward to compress the sheets with a velocity of 0.5 mm/s. The sheets underwent large deformation in the space surrounded by the sliding sectors. A mechanical interlock was produced between the two AL6061-T4 sheets to hook the sheets together. The clinched joint with a bottom thickness of 1.3 mm was produced by controlling the displacement of the punch.

5.2.3 Reshaping process with a rivet

The clinched joint was reshaped to increase the static strength in the reshaping process with a rivet. The rivet is shown in Fig. 5.5. The reshaping process was carried out on a hydraulic servo press. The velocity, displacement and force of the hydraulic servo press can be controlled precisely. A protrusion and a pit on the clinched joint were produced in the mechanical clinching process. A rivet was placed in the pit of the clinched joint. The material of the rivet is Al6061, which can be deformed in the reshaping process.

Fig. 5.5 Rivet

As shown in Fig. 5.6, two flat dies were used to compress the protrusion of the conventional mechanical clinched joint. The velocity of the top die was set to 0.05 mm/s. The rivet was used to support the clinched joint and control the material flow. When the protrusion height of the clinched joint was reduced to 1.0 mm, the top die was controlled to stop at once.

Fig. 5.6 Two flat dies

5.2.4 Reshaping process with no auxiliary

The clinched joint was reshaped to increase the static strength in the reshaping process with no auxiliary. The clinched joint was placed between the flat dies. The top flat die was controlled to move down to compress the clinched joint with a velocity of 0.05 mm/s. When the protrusion height of the clinched joint was reduced to 1.0 mm, the top die was controlled to stop at once.

5.2.5 Reshaping process with a bumped die

The clinched joint was reshaped to increase the static strength in the reshaping process with a bumped die. The bump on the bumped die was applied to support the clinched joint and control the material flow. The top flat die was used to compress the protrusion of the clinched joint with a velocity of 0.05 mm/s. The bumped die and the flat die are shown in Fig. 5.7. In order to compare the three reshaping methods equally, the reshaped joint with a bumped die also has a protrusion height of 1.0 mm.

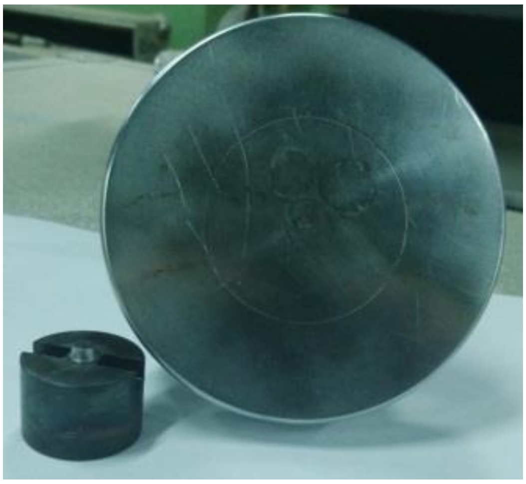

Fig. 5.7 The bumped die and flat die

5.3 Results and discussion

5.3.1 Reshaping force

Different dies and additional parts were used in the three reshaping processes. The reshaping forces of the different reshaped joints are different. The reshaping force-displacement curves of the reshaped joints produced by different reshaping methods are shown in Fig. 5.8.

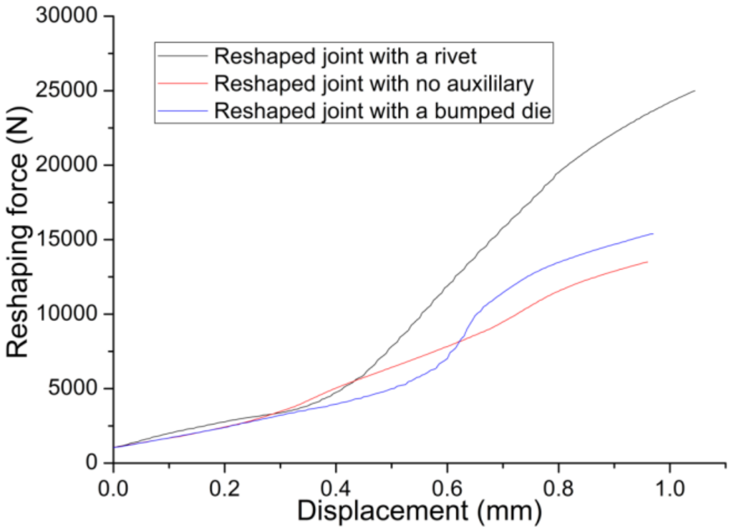

Fig. 5.8 The reshaping force-displacement curves

As can be seen, the maximum reshaping force of the reshaped joint with no auxiliary is the lowest, while the maximum reshaping force of the reshaped joint with a rivet is the highest. In the reshaping process with a rivet, the rivet is also compressed and deformed, so the reshaping force of the reshaped joint with a rivet is the highest. In the reshaping process with a bumped die, the bumped die may generate the resistance to the material flow of the protrusion, so the reshaping force of the reshaped joint with a bumped die is higher than that of the reshaped joint with no auxiliary.

5.3.2 Cross-tensile strength and energy absorption

The cross-tensile strength of the clinched joint is always lower than the tension-shearing strength. Many clinched joints lose efficiency because of a low cross-tensile strength. It is essential for the reshaping process to help the clinched joint increase the cross-tensile strength.

The average cross-tensile strength of five specimens for each test is taken as the evaluation index of the reshaped joint. The cross-tensile strengths of the clinched joint and the reshaped joints produced by different reshaping methods are shown in Table. 5.1.

Table 5.1 Cross-tensile strengths of the joints

Joint type	Average cross-tensile strength (N)
Clinched joint	908
Reshaped joint with a rivet	1052
Reshaped joint no auxiliary	943
Reshaped joint with a bumped die	970

As can be seen, the cross-tensile strength of the clinched joint is the lowest, while the cross-tensile strength of the reshaped joint with a rivet is the highest. All the reshaped joints have higher cross-tensile strength than the clinched joint. This proves that all the reshaping methods can increase the cross-tensile strength of the clinched joint.

The cross-tensile strength of the reshaped joint with a rivet is increased by 15.6% compared with the clinched joint. The cross-tensile strength of the reshaped joint with no auxiliary is increased by 3.9% compared with the clinched joint. The cross-tensile strength of the reshaped joint with a bumped die is increased by 6.8% compared with the clinched joint. The reshaping method with a rivet has the best performance for increasing the cross-tensile strength of the clinched joint.

The cross-tensile force-displacement curves of the clinched joint and reshaped joints with different reshaping methods are shown in Fig. 5.9. The cross-tensile force-displacement curve of the clinched joint undergoes smallest displacement before failure, and the cross-tensile force-displacement curve of the reshaped joint with a rivet undergoes largest displacement before failure. All the curves show a rising trend before the maximum curve peak, and all the curves drop rapidly after the maximum curve peak.

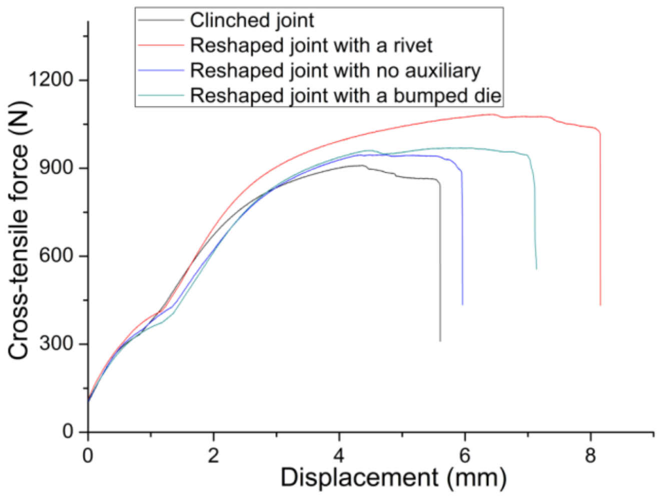

Fig. 5.9 The cross-tensile force-displacement curves of the joints

Another evaluation index of the clinched joint is the energy absorption in the static strength test. The ability of energy absorption represents the safety and reliability of the joint. Energy absorption of the joint can be gotten by measuring the area between the force-displacement curve and x-axis. It is better for the reshaped joint to have a high energy absorption in the cross-tensile strength test. The energy absorption values of the clinched joint and the reshaped joints with different reshaping methods in the cross-tensile strength tests are shown in Fig. 5.10.

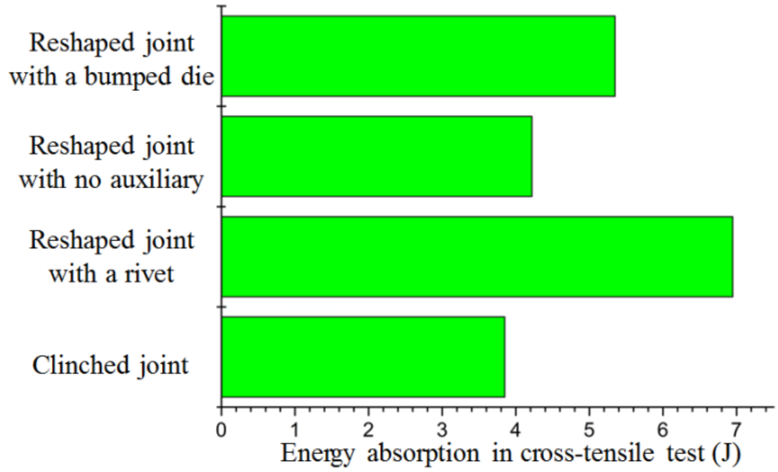

Fig. 5.10 Energy absorption values of the joints

As can be seen, all the reshaped joints have higher energy absorption than the clinched joint. The reshaped joint with a rivet has the highest energy absorption. All the reshaping methods can help the clinched joint to increase the energy absorption.

5.3.3 Tension-shearing strength and energy absorption

Tension-shearing condition is more representative for some applications of the clinched joint. It is essential for the reshaped joint to have a high tension-shearing strength. The average tension-shearing strength of five specimens for each test is taken as the evaluation index of the reshaped joint. The tension-shearing strengths of the clinched joint and the reshaped joints with different reshaping methods are shown in Table. 5.2.

Table 5.2 Tension-shearing strengths of the joints

Joint type	Average tension-shearing strength (N)
Clinched joint	1214
Reshaped joint with a rivet	2946
Reshaped joint with no auxiliary	1419
Reshaped joint with a bumped die	1533

As can be seen, all the reshaped joints have higher tension-shearing strength than the clinched joint. The reshaping methods can increase the tension-shearing strength of the clinched joint. The average tension-shearing strength of the reshaped joint with a rivet is 142.7% higher than that of the clinched joint. The average tension-shearing strength of the reshaped joint with no auxiliary is 16.9% higher than that of the clinched joint. The average tension-shearing strength of the reshaped joint with a bumped die is 26.3% higher than that of the clinched joint. The relative magnitude of the tension-shearing strengths of the reshaped joints is similar with that of the cross-tensile strengths.

The reshaped joint with a rivet has the highest tension-shearing strength. The rivet embedded in the pit of the joint can help the joint to bear the tension-shearing force in the tension-shearing strength test. So the tension-shearing strength of the reshaped joint with a rivet is the highest.

The tension-shearing force-displacement curves of the clinched joint and reshaped joints with different reshaping methods are shown in Fig. 5.11. All the curves show a rising trend before the maximum curve peak, and all the curves drop gradually after the maximum curve peak. The reshaped joint with a rivet has larger displacement before failure than other joints. The reshaping method with a rivet contributes to increase the displacement of the clinched joint before failure.

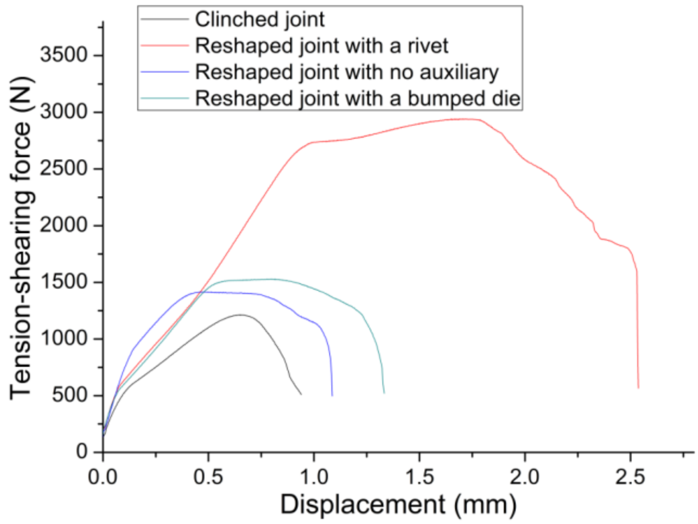

Fig. 5.11 The tension-shearing force-displacement curves of the joints

It is better for the reshaped joint to have a high energy absorption in the tension-shearing strength test. The energy absorption values of the clinched joint and the reshaped joints with different reshaping methods in the tension-shearing strength test are shown in Fig. 5.12.

As can be seen, the clinched joint has the lowest energy absorption in the tension-shearing test, while the reshaped joint with a rivet has the highest energy absorption. All the reshaped joints have higher energy absorption than the clinched joint. The relative magnitude of the energy absorption of the reshaped joints in the tension-shearing tests is similar with that of the energy absorption in the cross-tensile tests.

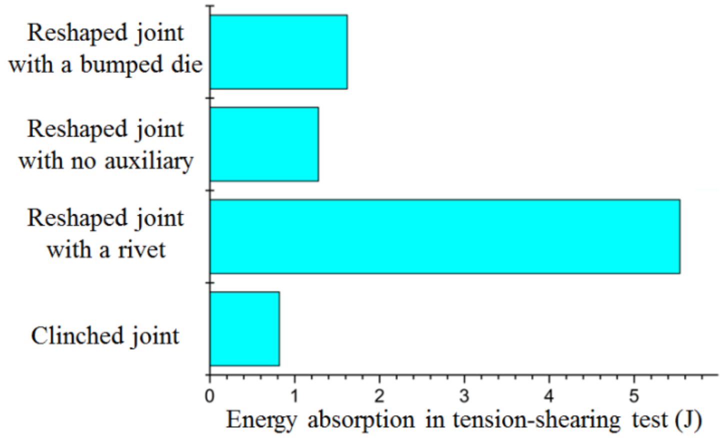

Fig. 5.12 Energy absorption values of the joints

5.3.4 Failure mode

In order to make sure that the joint has a high reliability, the failure mode of the joint should be investigated. There are two main failure modes of the clinched joint, neck fracture mode and button separation mode. The joint is fractured at the neck, which is named as neck fracture mode. The joint is separated with no fracture, which is named as button separation mode. A small neck may cause the neck fracture mode, and a small interlock may cause the button separation mode.

As can be seen from Fig. 5.13, the clinched joint and the reshaped joints failed as the neck fracture mode in the cross-tensile tests. This is because the maximum force which the neck of the joint can bear is lower than that which the interlock of the joint can bear. As can be seen from Fig. 5.14, the clinched joint and the reshaped joints also failed as the neck fracture mode in the tension-shearing tests. All the joints were fractured at the neck. As for the reshaped joint with a rivet, the rivet is not damaged, and it is still retained in the upper sheet. The failure mode of the joints is not changed by the reshaping methods.

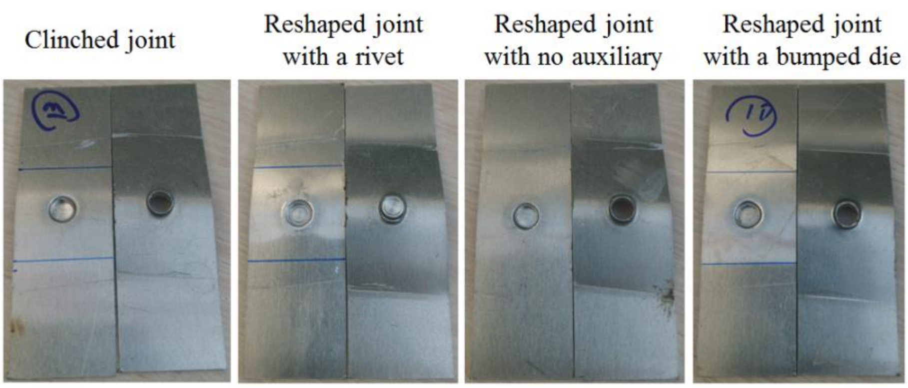

Fig. 5.13 Neck fracture mode in the cross-tensile tests

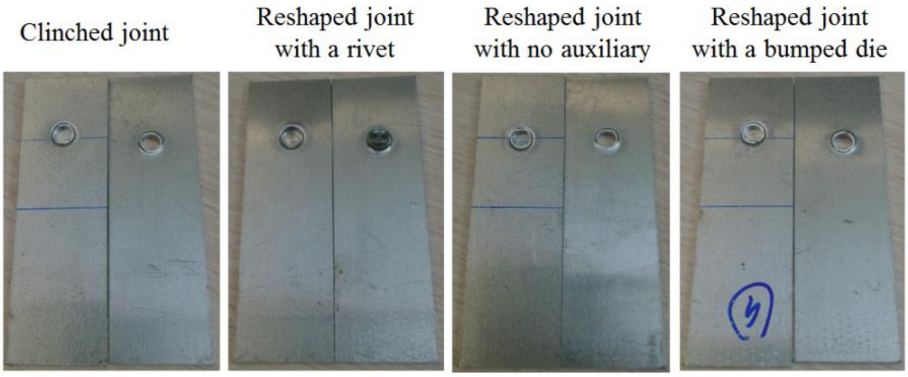

Fig. 5.14 Neck fracture mode in the tension-shearing tests

5.3.5 Neck thickness

As for the joint which fails as the button separation mode, the static strength of the joint is mainly determined by the interlock. As for the joint which fails as the neck fracture mode, the static strength of the joint is mainly determined by the neck thickness. In this study, all the joints failed as the neck fracture mode, which means that the neck thickness is the key geometrical parameter of the joint. The neck thicknesses of the clinched joint and reshaped joints with different reshaping methods are shown in Fig. 5.15.

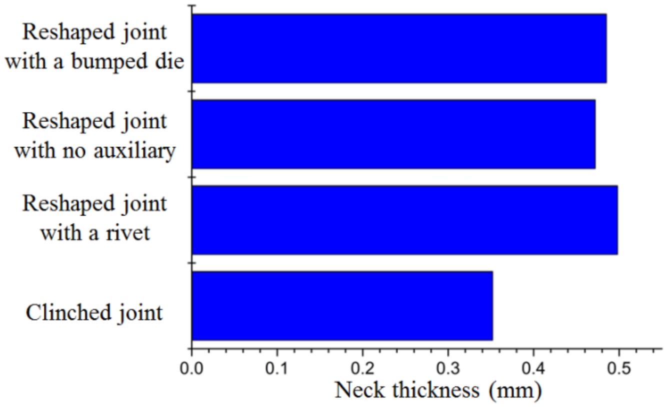

Fig. 5.15 Neck thicknesses of the joints

As can be seen, the clinched joint has the smallest neck thickness, while the reshaped joint with a rivet has the largest neck thickness. All the reshaping methods can increase the neck thickness of the clinched joint.

The trend of the cross-tensile strengths and tension-shearing strengths of the joints is similar with the trend of the neck thicknesses of the joints. This proves that the static strength of the reshaped joint is mainly determined by the neck thickness in this study. The reshaping method with a rivet has the best performance for increasing the neck thickness of the joint, so the reshaped joint with a rivet has the highest cross-tensile strength and tension-shearing strength.

The cross-sectional profiles of the different joints are shown in Fig. 5.16. In order to make the comparison easily, the clinched joint and reshaped joint are shown in the same figure. The left part of each figure shows the cross-sectional profile of the clinched joint, and the right part of each figure shows the cross-sectional profile of the reshaped joint. As can be seen, the mechanical interlocks are not damaged in the reshaping processes. The upper sheet and the bottom sheet are still joined together by the interlock. All the reshaped joints have lower protrusion height than the clinched joint.

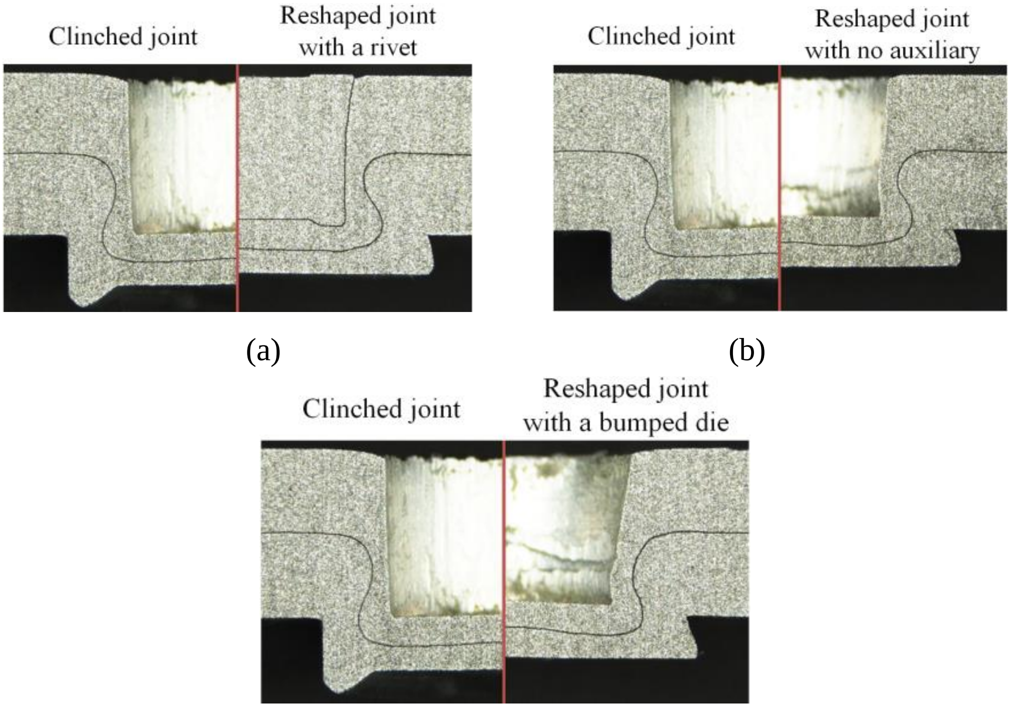

(a) (b)

(c)

Fig. 5.16 Cross-sectional profiles of the different joints: (a) reshaped joint with a rivet, (b) reshaped joint with no auxiliary, (c) reshaped joint with a bumped die

5.4 Conclusions

In order to increase the static strength of the clinched joint, three different reshaping methods were investigated and compared in the present work. The first reshaping method uses a rivet. The second reshaping method requires no auxiliary. The third reshaping method uses a bumped die. Reshaping force, cross-tensile strength, tension-shearing strength, energy absorption, failure mode and neck thickness of the joint were investigated. The main conclusions of the present work can be drawn as follows:

(1) The maximum reshaping force of the reshaped joint with no auxiliary is the lowest, while the maximum reshaping force of the reshaped joint with a rivet is the highest. The additional parts used in the reshaping process can increase the reshaping

force.

(2) The cross-tensile strength of the clinched joint is the lowest, while the cross-tensile strength of the reshaped joint with a rivet is the highest. All the reshaping methods can increase the cross-tensile strength of the clinched joint. The energy absorption of the joint in the cross-tensile test also can be increased by the three reshaping methods.

(3) All the reshaping methods can increase the tension-shearing strength of the clinched joint. The reshaping method with a rivet has the best performance for increasing the tension-shearing strength of the clinched joint. The energy absorption of the joint in the tensile-shearing test also can be increased by the three reshaping methods.

(4) Neck fracture mode is the main failure mode of the different joints. The failure mode of the clinched joint was not changed by the three reshaping methods.

(5) The clinched joint has the smallest neck thickness, while the reshaped joint with a rivet has the largest neck thickness. The strength of the joint was mainly influenced by the neck thickness. The three reshaping methods can increase the static strength and energy absorption of the joint by increasing the neck thickness.

6 Conclusions

In order to reduce the protrusion height and increase the strength of clinched joints, a two-steps clinching method using a rivet to reshape the clinched joint was put forward in the study. The reshaping method in the second step can be a helpful supplement of conventional mechanical clinching. The conclusions can be drawn as follows:

(1) The numerical results and experimental results are in good agreement, and the error in the evaluation of the cross-tensile strength is less than 1%. The best combination of the reshaping rivet geometrical parameters was gotten in terms of the cross-tensile strength by orthogonal design. Factor A and factor B have significant effects on cross-tensile strength and the order of the factors' importance is A (d_1), B (α_1), F (l_2), C (l_1), E (α_2), and D (d_2). In the experiment, when the protrusion height of the joint was reduced to 1.0 mm, the average cross-tensile strength was increased from 957.9 to 1154.9 N, and the average tension-shearing strength was increased from 1229.4 to 2757.3 N.

(2) Forming force is an important factor in the forming process. The neck thickness and interlock of the two-steps clinched joint are all larger than those of the clinched joint. The material flow in the reshaping process contributes to increase the strength and reduce the protrusion height of the clinched joint. The protrusion height of the two-steps clinched joint decreases with the increase of the reshaping force. The cross-tensile and tension-shearing strengths of the two-steps clinched joints with different reshaping forces are all higher than those of the conventional clinched joint. The cross-tensile and tension-shearing strengths of the two-steps clinched joint with a forming force of 35kN are the highest of all. Neck fracture mode is the main failure mode. Neck thickness has an important influence on the strength of the joint. The failure process of the two-steps clinched joint involves much higher energy absorption than the conventional clinched joint.

(3) The two-steps clinching process is suitable for joining different aluminum alloy sheets. The joint with an upper sheet of AL6061 and a lower sheet of AL5052 has higher strength than the joint with an upper sheet of AL5052 and a lower sheet of AL6061. The rivet can help the joint to increase the strength in the two-steps clinching process. The two-steps clinching process is suitable for joining aluminum alloy sheets with different thicknesses. The COJ2.5-2.0 joint has the highest strength, while the CLJ2.0-2.5 joint has the lowest strength. For joining aluminum alloy sheets with different thicknesses, it is better to take the thicker sheet as the upper sheet to get

a higher strength. The two-steps clinched joint with a bottom thickness of 1.6 mm has the highest cross-tensile strength and tension-shearing strength among the two-steps clinched joints in case of the joints with bottom thicknesses of 1.4, 1.5, and 1.6 mm.

(4) The maximum reshaping force of the reshaped joint with no auxiliary is the lowest, while the maximum reshaping force of the reshaped joint with a rivet is the highest. The additional parts used in the reshaping process can increase the reshaping force. The cross-tensile strength of the clinched joint is the lowest, while the cross-tensile strength of the reshaped joint with a rivet is the highest. All the reshaping methods can increase the cross-tensile strength of the clinched joint. The energy absorption of the joint in the cross-tensile test also can be increased by the three reshaping methods. All the reshaping methods can increase the tension-shearing strength of the clinched joint. The reshaping method with a rivet has the best performance for increasing the tension-shearing strength of the clinched joint. The energy absorption of the joint in the tensile-shearing test also can be increased by the three reshaping methods. Neck fracture mode is the main failure mode of the different joints. The failure mode of the clinched joint was not changed by the three reshaping methods. The clinched joint has the smallest neck thickness, while the reshaped joint with a rivet has the largest neck thickness. The strength of the joint was mainly influenced by the neck thickness. The three reshaping methods can increase the static strength and energy absorption of the joint by increasing the neck thickness.

Reference

[1] Delogu, M., Zanchi, L., Maltese, S., Bonoli, A., Pierini, M., 2016. Environmental and Economic Life Cycle Assessment of a lightweight solution for an automotive component: A comparison between talc-filled and hollow glass microspheres-reinforced polymer composites. J. Clean. Prod. 139, 548-560.

[2] Fan, Y., Peng, B. B., Xu, J. H., 2017. The effect of technology adoption on CO 2 abatement costs under uncertainty in China's passenger car sector. J. Clean. Prod. 154, 578-592.

[3] Danilecki, K., Mrozik, M., Smurawski, P., 2017. Changes in the environmental profile of a popular passenger car over the last 30 years–Results of a simplified LCA study. J. Clean. Prod. 141, 208-218.

[4] Zhou, J., Wang, F., Wan, X., 2015. Optimal design and experimental investigations of Aluminum sheet for lightweight of car hood. Materials Today: Proceedings, 2(10), 5029-5036.

[5] Abe, Y., Kato, T., Mori, K. I., Nishino, S., 2014. Mechanical clinching of ultra-high strength steel sheets and strength of joints. J. Mater. Process. Technol. 214(10), 2112-2118.

[6] Abe, Y., Mori, K., Kato, T., 2012. Joining of high strength steel and aluminum alloy sheets by mechanical clinching with dies for control of metal flow. J. Mater. Process. Technol. 212(4), 884-889.

[7] Lambiase, F., Di Ilio, A., 2013. Finite element analysis of material flow in mechanical clinching with extensible dies. J. Mater. Eng. Perform. 22(6), 1629-1636.

[8] Abe, Y., Saito, T., Mori, K. I., Kato, T., 2017. Mechanical clinching with dies for control of metal flow of ultra-high-strength steel and high-strength steel sheets. Proc. IMechE. Part B: J. Engineering. Manufacture. DOI: 10.1177/0954405416683429.

[9] He, X., 2017. Clinching for sheet materials. Sci. Technol. Adv. Mat. 18(1), 381-405.

[10] Coppieters, S., Lava, P., Baes, S., Sol, H., Van Houtte, P., Debruyne, D., 2012. Analytical method to predict the pull-out strength of clinched connections. Thin. Wall. Struct. 52, 42-52.

[11] Coppieters, S., Lava, P., Sol, H., Van Bael, A., Van Houtte, P., Debruyne, D., 2010. Determination of the flow stress and contact friction of sheet metal in a multi-layered upsetting test. J. Mater. Process. Technol. 210(10), 1290-1296.

[12] Lambiase, F., 2013. Influence of process parameters in mechanical clinching with extensible dies. Int. J. Adv. Manuf. Technol. 66, 2123-2131.

[13] Lee, C.J., Kim, J.Y., Lee, S.K., Ko, D.C., Kim, B.M., 2010. Design of mechanical clinching tools for joining of aluminum alloy sheets. Mater. Des. 31, 1854-1861.

[14] Oudjene, M., Ben-Ayed, L., 2008. On the parametrical study of clinch joining of metallic sheets using the taguchi method. Eng. Struct. 30, 1782-1788.

[15] Oudjene, M., Ben-Ayed, L., Delamézière, A., Batoz, J.L., 2009. Shape optimization of clinching tools using the response surface methodology with Moving Least-Square approximation. J. Mater. Process. Technol. 209, 289-296.

[16] Han, X., Zhao, S., Liu, C., Chen, C., Xu, F., 2016. Optimization of geometrical design of clinching tools in clinching process with extensible dies. Proc. IMechE. Part. C: J. Mechanical. Engineering. Science. DOI:10.1177/0954406216660336.

[17] He, X., 2010. Recent development in finite element analysis of clinched joints. Int. J. Adv. Manuf. Technol.48(5), 607-612.

[18] Wen, T., Wang, H., Yang, C., Liu, L.T., 2014. On a reshaping method of clinched joints to reduce the protrusion height. Int. J. Adv. Manuf. Technol. 71(9-12), 1709-1715.

[19] He, X., Zhao, L., Yang, H., Xing, B., Wang, Y., Deng, C., Ball, A., 2014. Investigations of strength and energy absorption of clinched joints. Comp. Mater. Sci. 94, 58-65.

[20] He, X., Liu, F., Xing, B., Yang, H., Wang, Y., Gu, F., Ball, A., 2014. Numerical and experimental investigations of extensible die clinching. Int. J. Adv. Manuf. Technol. 74(9-12), 1229-1236.

[21] Hamel, V., Roelandt, J. M., Gacel, J. N., Schmit, F., 2000. Finite element modeling of clinch forming with automatic remeshing. Comput. Struct. 77(2), 185-200.

[22] Coppieters, S., Cooreman, S., Lava, P., Sol, H., Van Houtte, P., Debruyne, D., 2011. Reproducing the experimental pull-out and shear strength of clinched sheet metal connections using FEA. Int. J. Mater. Form. 4(4), 429-440.

[23] Lambiase, F., Ko, D.C., 2016. Feasibility of mechanical clinching for joining aluminum AA6082-T6 and carbon fiber reinforced polymer sheets. Mater. Des. 107, 341-352.

[24] Zhao, S.D., Xu, F., Guo, J.H., Han, X.L., 2014. Experimental and numerical research for the failure behavior of the clinched joint using modified Rousselier model. J. Mater. Process. Technol. 214(10), 2134-2145.

[25] He, X., Zhang, Y., Xing, B., Gu, F., Ball, A., 2015. Mechanical properties of extensible die clinched joints in titanium sheet materials. Mater. Des. 71, 26-35.

[26] Meschut, G., Janzen, V., Olfermann, T., 2014. Innovative and highly productive joining technologies for multi-material lightweight car body structures. J. Mater. Eng. Perform. 23, 1515-1523.

[27] Hörhold, R., Müller, M., Merklein, M., Meschut, G., 2016. Mechanical properties of an innovative shear-clinching technology for ultra-high-strength steel and aluminum in lightweight car body structures. Weld. World. 60(3), 613-620.

[28] Lambiase, F., Ko, D.C., 2016. Feasibility of mechanical clinching for joining aluminum AA6082-T6 and carbon fiber reinforced polymer sheets. Mater. Des. 107, 341-352.

[29] Lambiase, F., 2015. Mechanical behaviour of polymer–metal hybrid joints produced by clinching using different tools. Mater. Des. 7(15), 606-618.

[30] Lambiase, F., Durante, M., Di Ilio, A., 2016. Fast joining of aluminum sheets with Glass Fiber Reinforced Polymer (GFRP) by mechanical clinching. J. Mater. Process. Technol. 236, 241-251.

[31] Lambiase, F., 2015. Joinability of different thermoplastic polymers with aluminum AA6082 sheets by mechanical clinching. Int. J. Adv. Manuf. Technol. 80(9), 1995-2006.

[32] Lambiase, F., Di Ilio. A., 2015. Mechanical clinching of metal–polymer joints. J. Mater. Process. Technol. 215, 12-19.

[33] Saberi, S., Enzinger, N., Vallant, R., Cerjak, H., Hinterdorfer, J., Rauch, R., 2008. Influence of plastic anisotropy on the mechanical behavior of clinched joint of different coated thin steel sheets. Int. J. Mater. Form. 1, 273-276.

[34] Abe, Y., Kishimoto, M., Kato, T., Mori, K., 2009. Joining of hot-dip coated steel sheets by mechanical clinching. Int. J. Mater. Form. 2, 291-294.

[35] Jiang, T., Liu, Z.X., Wang, P.C., 2015. Effect of aluminum pre-straining on strength of clinched galvanized SAE1004 steel-to-AA6111-T4 aluminum. J. Mater. Process. Technol. 215, 193-204.

[36] Lambiase, F., Di Ilio, A., Paoletti, A., 2015. Joining aluminum alloys with reduced ductility by mechanical clinching. Int. J. Adv. Manuf. Technol. 77(5-8), 1295-1304.

[37] Lambiase, F., Ko, D.C., 2016. Feasibility of mechanical clinching for joining aluminum AA6082-T6 and carbon fiber reinforced polymer sheets. Mater. Des. 107, 341-352.

[38] Breda, A., Coppieters, S., Debruyne, D., 2017. Equivalent modelling strategy for

a clinched joint using a simple calibration method. Thin. Wall. Struct. 113, 1-12.
[39] Lambiase, F., 2015c. Clinch joining of heat-treatable aluminum AA6082-T6 alloy under warm conditions. J. Mater. Process. Technol. 225, 421-432.
[40] Lambiase, F., Paoletti, A., Di Ilio, A., 2017. Advances in Mechanical Clinching: Employment of a Rotating Tool. Procedia Engineering, 183, 200-205.
[41] Kim, H. K., 2013. Fatigue strength evaluation of the clinched lap joints of a cold rolled mild steel sheet. J. Mater. Eng. Perform. 22(1), 294-299.
[42] Mori, K., Abe, Y., Kato, T., 2012. Mechanism of superiority of fatigue strength for aluminum alloy sheets joined by mechanical clinching and self-pierce riveting. J. Mater. Process. Technol. 212(9), 1900-1905.
[43] Neugebauer, R., Todtermuschke, M., Mauermann, R., Riedel, F., 2008. Overview on the state of development and the application potential of dieless mechanical joining processes. Arch. Civ. Mech. Eng. 8(4), 51-60.
[44] Gerstmann, T., Awiszus, B., 2014. Recent developments in flat-clinching. Comp. Mater. Sci. 81, 39-44.
[45] Han, X., Zhao, S., Chen, C., Liu, C., Xu, F., 2016. Optimization of geometrical design of clinching tools in flat-clinching. Proc. IMechE. Part. C: J. Mechanical. Engineering. Science. DOI: 10.1177/0954406216660335.
[46] Härtel, S., Graf, M., Gerstmann, T., Awiszus, B. 2017. Heat Generation During Mechanical Joining Processes–by the Example of Flat-Clinching. Procedia. Engineering. 184, 251-265.
[47] Lüder, S., Härtel, S., Binotsch, C., Awiszus, B. 2014. Influence of the moisture content on flat-clinch connection of wood materials and aluminum. J. Mater. Process. Technol. 214(10), 2069-2074.
[48] Lee, C. J., Lee, S. H., Lee, J. M., Kim, B. H., Kim, B. M., Ko, D. C., 2014. Design of hole-clinching process for joining CFRP and aluminum alloy sheet. Int. J. Precis. Eng. Man. 15(6), 1151-1157.
[49] Lee, C.J., Lee, J.M., Ryu, H.Y., Lee, K.H., Kim, B.M., Ko, D.C., 2014. Design of hole-clinching process for joining of dissimilar materials–Al6061-T4 alloy with DP780 steel, hot-pressed 22MnB5 steel, and carbon fiber reinforced plastic. J. Mater. Process. Technol. 214(10), 2169-2178.
[50] Lee, C. J., Kim, B. M., Kang, B. S., Song, W. J., Ko, D. C., 2017. Improvement of joinability in a hole clinching process with aluminum alloy and carbon fiber reinforced plastic using a spring die. Compos. Struct. 173, 58-69.
[51] Wen, T., Huang, Q., Liu, Q., Ou, W. X., Zhang, S., 2016. Joining different metallic sheets without protrusion by flat hole clinching process. Int. J. Adv. Manuf. Technol. 85(1-4), 217-225.

[52] de Paula, A.A., Aguilar, M.T.P, Pertence, A.E.M, Cetlin, P.R., 2007. Finite element simulations of the clinch joining of metallic sheets. Journal of Materials Processing Technology 182 (1-3), 352-357.

[53] Mucha, J., Witkowski, W., 2014. The clinching joints strength analysis in the aspects of changes in the forming technology and load conditions. Thin-Walled Struct 82, 55-66.

Research papers of this research

学術雑誌

【主論文】

1)“Effects of geometrical parameters on the strength and energy absorption of the height-reduced joint”
Chao Chen, Shengdun Zhao, Minchao Cui, Xiaolan Han, Xuzhe Zhao, Tohru Ishida.
International Journal of Advanced Manufacturing Technology, Vol. 90, Page 3533-3541, June, 2017. Published

2) “Comparative study on two compressing methods of clinched joints with dissimilar aluminum alloy sheets”
Chao Chen, Xiaolan Han, Shengdun Zhao, Fan Xu, Xuzhe Zhao, Tohru Ishida.
International Journal of Advanced Manufacturing Technology, Vol. 93, Page 1929-1937, November, 2017. Published

3) “Experimental investigation of the mechanical reshaping process for joining aluminum alloy sheets with different thicknesses”
Chao Chen, Shengdun Zhao, Xiaolan Han, Minchao Cui, Xuzhe Zhao, Tohru Ishida.
Journal of Manufacturing Processes, Vol. 26, Page 105-112, April, 2017. Published

4) “An experimental study on the compressing process for joining Al6061 sheets”
Chao Chen, Shengdun Zhao, Minchao Cui, Xiaolan Han, Shuqin Fan, Tohru Ishida.
Thin-walled Structures, Vol. 108, Page 56-63, November, 2016. Published

5) “Experimental investigation on the joining of aluminum alloy sheets using improved clinching process”
Chao Chen, Shengdun Zhao, Xiaolan Han, Xuzhe Zhao, Tohru Ishida.
Materials, Vol. 10, No.887, August, 2017. Published

6) “Experimental study on the height-reduced joints to increase the cross-tensile strength”
Chao Chen, Shuqin Fan, Xiaolan Han, Shengdun Zhao, Minchao Cui, Tohru Ishida.
International Journal of Advanced Manufacturing Technology, Vol. 91, Page 2655-2662, July, 2017. Published

7) “Influence of sheet thickness on mechanical clinch-compress joining technology”
Chao Chen, Xiaolan Han, Shengdun Zhao, Fan Xu, Xuzhe Zhao, Tohru Ishida.
Proceedings of the Institution of Mechanical Engineers, Part E: Journal of Process Mechanical Engineering, DOI: 10.1177/0954408917735717, October, 2017. Published

8) “Experimental research on the compressed joints with different geometrical

parameters"
Chao Chen, Shuqin Fan, Xiaolan Han, Shengdun Zhao, Minchao Cui, Tohru Ishida.
Proceedings of the Institution of Mechanical Engineers, Part B: Journal of Engineering Manufacture, DOI: 10.1177/0954405417711735, June, 2017. Published online

【副論文】

国際会議
9) "Numerical and experimental investigations of the two-step clinching process."
Chao Chen, Tohru Ishida, Shengdun Zhao, Xiaolan Han, Xuzhe Zhao.
International Conference on Design and Concurrent 2017 & Manufacturing Systems Conference 2017, September 7-8, Osaka, Japan

Acknowledgement

It is a significant and unforgettable experience for me to spend such a long time on writing, modifying and polishing this thesis. Many kind-hearted people give me a great amount of help, professional advice and encouragement. Thus, here I would like to express my sincere gratitude to them.

First of all, I will show my sincere thanks to my supervisor, Prof. Ishida, who has given me invaluable guidance and constant support and encouragement throughout the whole processes. Prof. Ishida is knowledgeable, sagacious, kindly, responsible, and friendly. During my study of mechanical engineering in this two years and the witting of this thesis, he has always been generous to offer me useful suggestions, answer my question and discuss research questions with me. His detail guidance and helpful comments on my thesis encourage me to overcome difficulties and think more critically during the processes of writing. During my study in Japan, he gave me a lot of help. With his support, I published many papers and achieved good academic achievements.

Secondly, I will also express my sincere gratitude to other professor and teachers, such as Prof. Shengdun Zhao, Prof. Mizobuchi and Dr. Sanusi, who had given me constructive suggestion to my study and thanks to them for instructing me to construct my knowledge in mechanical engineering in the past two years.

Thirdly, I want to thank all my affectionate classmates and friends, such as Ogawa san, Sato san, Kimiharu san, Minchao Cui, Zifan Miao and so on. During the two years' study, they have given me a lot of support and encouragement in their own ways.

At last, I will give the deepest gratitude to my family for their regretless support and love to me.